Journal
of
The Franklin Institute

EDITOR, HENRY BUTLER ALLEN, MET.E., D.Sc.
ASSISTANT EDITOR, JOHN FRAZER, PH.D.

Associate Editors:

WILDER D. BANCROFT, PH.D. — A. S. EVE, F.R.S. — HENRY C. SHERMAN, SC.D.
C. B. BAZZONI, PH.D. — PAUL D. FOOTE, PH.D. — W. F. G. SWANN, D.SC.
E. G. COKER, F.R.S. — W. J. HUMPHREYS, PH.D. — HUGH S. TAYLOR, D.SC.
ARTHUR L. DAY, SC.D. — C. E. K. MEES, D.SC. — A. F. ZAHM, PH.D.
R. EKSERGIAN, PH.D. — WILLIAM B. MELDRUM, PH.D. — JOHN ZELENY, PH.D.

Committee on Publications:

G. H. CLAMER, CHAIRMAN — LIONEL F. LEVY — HIRAM S. LUKENS
RICHARD HOWSON — MALCOLM LLOYD, JR. — RICHARD H. OPPERMANN
C. L. JORDAN — WINTHROP R. WRIGHT

Vol. 240 — **NOVEMBER, 1945** — **No. 5**

CONTENTS

The Transient Performance of Propellers and Ships During Backing and Reversal. II. REINHOLD RÜDENBERG 347

Circulation in Sanitary Ventilation by Bactericidal Irradiation of Air . . W. F. WELLS 379

The Electrical Constants of the Electromagnetic Microbarograph. EUGENE L. SULKOWSKI 397

Simplified Equations of Interior Ballistics . . . . . JOSEPH E. MAYER AND B. I. HART 401

Notes from the National Bureau of Standards 413

The Franklin Institute Notes 419

Notes from the Biochemical Research Foundation 422

Studies on the Chemotherapy of Experimental Virus Infections, II. DONALD W. MCKINSTRY AND ELIZABETH H. READING

Publications Received 430

Current Topics 396, 412, 431

Published by
THE FRANKLIN INSTITUTE OF THE STATE OF PENNSYLVANIA
Prince and Lemon Streets, Lancaster, Penna., and
Benjamin Franklin Parkway at Twentieth St., Philadelphia, Penna.

SIX DOLLARS PER YEAR (Foreign Postage Additional) **SINGLE NUMBERS, SIXTY CENTS**

Indexes to the semi-annual volumes of the JOURNAL are published with the June and December numbers. The contents are also indexed in *The Industrial Arts Index*.

PHILCO

Farm Radio!

A new *Philco* who brought to the farm homes of America new convenience and economy of A. C. radios by developing the sensational 10-Volt Battery Set. No wonder old people of our hospitals, clinics and therapeutic equipment many eliminated. Another example of Philco progressive that will bring new radio joy for the future of America.

Journal
of
The Franklin Institute
Devoted to Science and the Mechanic Arts

Vol. 240 NOVEMBER, 1945 No. 5

THE TRANSIENT PERFORMANCE OF PROPELLERS AND SHIPS DURING BACKING AND REVERSAL.

BY

REINHOLD RÜDENBERG,

Gordon McKay Professor of Electrical Engineering,
Graduate School of Engineering, Harvard University, Cambridge, Massachusetts.

PART II.

CONTENTS.

PAGE

6. Transient Performance of the Propeller Water..... 347
7. Transient Propeller Thrust..... 352
8. Pressure Drop and Cavitation..... 355
Appendix 1. Influence of the Forward Wake..... 363
Appendix 2. Contraction of the Propeller Wake..... 371

6. TRANSIENT PERFORMANCE OF THE PROPELLER WATER.

In part I, the forces of acceleration or deceleration, occurring within the propelling water when changing its velocity as a whole, have not been considered in detail. However, these forces, represented by the first term [15] on the right-hand side of eq. (3), play a dominant role during the backing and reversing processes of the propeller, qualitatively as well as quantitatively. They appear every time that one streamline diagram of Figs. 3–10 passes over into another. Since the ship velocity during any time element of retardation of the propeller changes only slightly, we may consider the superposed water velocity V as constant, and thus all accelerating forces now to be considered can be derived merely from a change in the velocities of the stationary streamline diagram Fig. 2, in which on the front side of the propellor the water is sucked in from all directions, while on the rear side it is expelled in a unidirectional jet.

The entire mechanism of the reversal of a ship during the transient period consists of a succession of forces acting on a number of inertia masses: (1) the motor develops a torque around the propeller shaft;

(Note—The Franklin Institute is not responsible for the statements and opinions advanced by contributors in the JOURNAL.)

(2) the rotational masses of motor and propeller become decelerated or accelerated; (3) the change of speed of the propeller produces an axial increment or decrement of force on the surrounding water, sucking on the inflow and pressing on the outflow, or inversely, as the case may be; (4) the masses of the water axially coupled with the propeller accelerate or decelerate from their former motion into a new one; (5) this effects an axial force of reaction on the propeller driving or backing the ship; (6) the ejection of a unilateral column out of the accelerated or retarded water surrounding the propeller exerts an axial force on the vessel via the propeller and its shaft; (7) the inertia masses of the vessel are accelerated or retarded under the axial forces of the propeller; (8) simultaneously with (4), the water is revolved by effect of the propeller blades, but the change of its rotational energy is only small compared with the translatory change.

In the former sections of this paper we have considered the acceleration of the motor and propeller according to items (1) and (2), and of the vessel according to item (7), under their respective forces and inertias. We will now analyze in detail the accelerating and retarding forces according to items (3) to (6), produced by the change of the water velocities in the space surrounding the propeller, if the water flow develops as shown by the streamlines of Fig. 2.

At first we consider a rotational acceleration of the propeller from the quiescent state, without axial movement of the propeller proper. Since every jet formation is initiated by the cumulative effects in time of viscosity and vorticity, as shown long ago by L. Prandtl,[6] at the first instant the water surrounding the propeller disk will behave like an ideal liquid. Thus under the axial forces of the starting propeller an annular vortex is formed around the rim of the propeller plane, the streamlines of which are shown in Fig. 24. It is well known [2] that the kinetic energy of the entire water moving in such a ring-vortex produced by a pressure difference over a circular disk of diameter d is given by

$$E = \frac{\rho d^3}{3} \cdot \frac{v^2}{2}, \tag{50}$$

where v is the uniform velocity at the surfaces of the disk. The first quotient in this equation obviously gives the equivalent inertia mass of the water surrounding the propeller, namely

$$m_w = \frac{\rho}{3} d^3 = \rho \frac{\pi d^2}{4} l. \tag{51}$$

On the right hand side this mass is expressed in terms of a cylinder of water of diameter d and length l, as shown in Fig. 24. Thus the equivalent axial length of a water cylinder through the propeller, containing

the same inertia as the ring-vertex, is

$$l = \frac{4}{3\pi} d = 0.425d. \tag{52}$$

Hence, during the starting of the propeller an inertia mass of water equivalent to a cylinder of propeller diameter d and axial length of almost half the diameter must be accelerated before a jet can be formed and a continuous thrust on the ship can be sustained. Since the inertia of such a water mass is comparable to the inertia of the rotating motor and propeller, this leads to a considerable increase of the effective time constant τ of the rotating parts, which governs, according to section 4, the reversal of the propeller in actual operation.

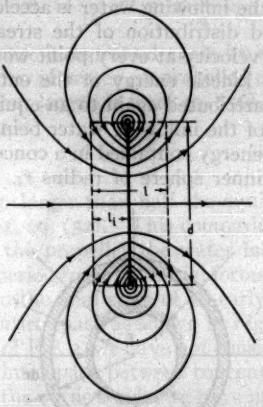

FIG. 24. Streamline pattern of propeller vortex formed during transient performance of propeller.

By action due to the viscosity of the water, after some time the ring-vortex shown in Fig. 24 moves in the direction of the water flow, changes gradually in shape, and constitutes finally the vortex cylinder forming the surface of the water column ejected from the propeller disk. In this way a streamline pattern as in Fig. 2 gradually develops from quiescent water.

There is not much known about the phenomena in detail, occurring during the continued acceleration of a water jet in the open water space. However, for the outflow side of the propeller it is certain that an acceleration of the water in the propeller disk will not simultaneously change the speed of the entire length of the column, and the same is true during retardation. Rather the increase of water velocity will extend only over the spatial increment of the column adjacent to the propeller disk, and from here on a new jet with higher velocity will be

formed which displaces itself in time through the water of the former column. Thus every accelerating step concerns at first only the water in contact with and immediately around the propeller disk and therefore an additional or incremental vortex as in Fig. 24 will be formed. This elemental ring-vortex at first is superposed on the previous column and finally merges with the surface of the new column of changed velocity. The same will be true also during retardation of the propeller. Hence, the incremental energy and the equivalent mass of the accelerated or decelerated water will correspond entirely to eqs. (50) and (51).

On the inflow side of the propeller, extending as in Fig. 2 from the propeller disk into the entire space not covered by the jet, the phenomena will be similar. However, here an alternative may be considered, namely that the inflowing water is accelerated or retarded as a whole with unchanged distribution of the streamlines. Then in the diagram of Fig. 2 the velocity at every point would gradually increase, thereby changing the kinetic energy of the entire inflowing water, a process which can be attributed again to an equivalent inertia mass.

The main motion of the inflowing water being radial, we can easily determine the kinetic energy contained in a concentric inflow, as shown in Fig. 25, up to an inner sphere of radius r_i. The mass element is

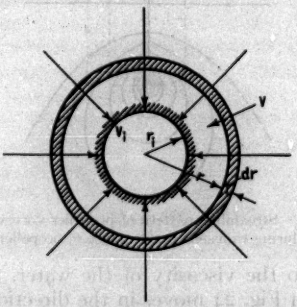

FIG. 25. Concentric inflow of propeller water towards a sink.

given by a concentric shell of radius r and thickness dr and the velocity is inversely proportional to the square of the radius, being v_i at the spherical sink. Thus the kinetic energy is

$$E_i = \int_{r_i}^{\infty} dm \frac{v^2}{2} = \int_{r_i}^{\infty} 4\pi\rho r^2 dr \cdot \left(\frac{r_i}{r}\right)^4 \cdot \frac{v_i^2}{2} = 4\pi\rho r_i^3 \cdot \frac{v_i^2}{2}. \quad (53)$$

The equivalent inertia mass of the inflowing water, related to the maximum velocity v_i, is evidently

$$m_i = 4\pi\rho r_i^3. \quad (54)$$

Hence the inertia of water flowing concentrically into a sink of radius r, is equal to three times the inertia of a water sphere with radius of the sink.

Actually the inflowing water in Fig. 2 does not converge towards a sphere but towards the plane propeller disk of diameter d, at which it attains its full velocity. We substitute therefore, as an approximation, the area of the propeller disk for the surface of the sphere, obtaining

$$\frac{\pi d^2}{4} = 4\pi r_i^2, \quad \text{or} \quad r_i = \frac{d}{4}, \tag{55}$$

and thus the equivalent mass of the entire inflowing water becomes

$$m_i = \frac{\pi}{16}\rho d^3 = \rho\frac{\pi d^2}{4} l_i. \tag{56}$$

In the last term the mass is expressed again by an equivalent length l_i of an inflowing cylinder of water of propeller area, indicated also in Fig. 24. The equivalent length is from eq. (56),

$$l_i = \frac{d}{4}, \tag{57}$$

which is 17.5 per cent. larger than half the equivalent cylinder length of the total ring-vortex, eq. (52). This comparison shows that at least on the inflow side of the propeller the water inertia increases slightly during the transition period from the initial formation of the ring-vortex shown in Fig. 24 up to the final state of a nearly concentric inflow and covering almost the entire space as shown in Fig. 2.

On the inflow side of Fig. 2, we have not considered in our derivation the movement in the interspace between concentric and unilateral flow into the propeller; on the outflow side, we have not covered the rotation of the water; actually both contribute further to the inertia. Hence, it seems safe to use for the actual inertia of the accelerated or decelerated propeller water an equivalent inertia cylinder over the propeller plane, having, instead of eq. (52), at least twice the length of eq. (57), namely

$$l = \frac{d}{2}. \tag{58}$$

The best conception of the quantitative significance of the inertia of the propeller water is obtained by determining its starting time constant τ_w. This magnitude is generally given by eq. (35), and if we substitute therein for the normal thrust T_n its value from eq. (6), and for the mass m_w a cylinder of propeller disk area A and length l, we obtain

$$\tau_w = \frac{U_n}{T_n} m_w = \frac{U_n}{\frac{\rho}{k^2} A U_n W_n} \rho A l = \frac{kl}{W_n} = \frac{kl}{s_n V_n}. \tag{59}$$

Hence, in view of eqs. (52) or (58), this time constant is directly proportional to the propeller diameter and inversely proportional to the normal slip and the ship's velocity, but it is not dependent on the many other parameters of the propulsion.

Numerically, we have, with $k = 0.8$ for a propeller of $d = 5$ *m.* diameter, driving a vessel with a slip of $s_n = 20$ per cent., at a velocity $V_n = 20$ kn. $= 10.3$ *m./sec.*, a water time constant of the propeller

$$\tau_w = \frac{0.8 \cdot 2.5}{0.2 \cdot 10.3} = 0.97 \text{ sec.}$$

Since the propeller diameter and therefore the length l of the inertia cylinder are larger for ships with higher velocity V_n, the water time constant of eq. (59) remains in the same order of magnitude for vessels of a similar type.

7. TRANSIENT PROPELLER THRUST.

The starting time constant of the propeller proper is given by the left-hand side of eq. (35) with moment of inertia I_p of the propeller, while the time constant of the propeller water was given by the right-hand side of the same equation with water mass m_w. Therefore, the ratio of both time constants is

$$\frac{\tau_p}{\tau_w} = \frac{I_p \omega_n / Q_n}{m_w U_n / T_n} = \frac{I_p}{m_w} \left(\frac{2\pi}{p} \right)^2 \frac{\eta'}{\eta''}. \tag{60}$$

On the right-hand side of this equation there are substituted for the quotients ω_n/Q_n and U_n/T_n the values according to eqs. (45) and (46). Considering Fig. 26, we can express the moment of inertia of a propeller

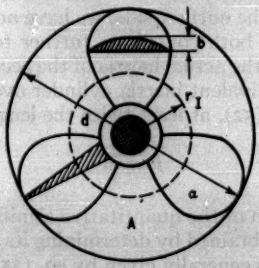

FIG. 26. Principal dimensions of propeller blades.

by its mass and the radius of gyration r_I, the former being given by the product of density ρ_p, area a and mean thickness b of the blades. The propeller water mass, on the other hand, is determined by area A of the propeller disk and equivalent inertia length l, given by eq. (58).

Thus the ratio of the moment of inertia of the propeller to the inertia mass of the propeller water becomes

$$\frac{I_p}{m_w} = \frac{\rho_p b a r_I^2}{\rho l A}. \tag{61}$$

Substituted into eq. (60), we obtain as ratio of the time constants of propeller and water

$$\frac{\tau_p}{\tau_w} = 4\pi^2 \frac{\rho_p}{\rho} \frac{b}{l} \frac{a}{A} \left(\frac{r_I}{p}\right)^2 \frac{\eta'}{\eta''}. \tag{62}$$

Because of the actual distribution of masses within the propeller blades, the radius of gyration will be of the order of 1/4 of the propeller diameter; the propeller diameter, on the other hand, is on the average about 80 per cent. of the propeller pitch. Thus we have a mean ratio

$$\frac{r_I}{p} = \frac{r_I}{d} \cdot \frac{d}{p} = \frac{1}{4} \cdot 0.8 = 0.2.$$

If we take as an example the density of the propeller metal $\rho_p/\rho = 8$, the mean blade thickness $b = 5$ *cm* for a propeller of 5 *m* diameter, having an equivalent inertia length $l = 2.5$ *m*, if the blades cover an area $a/A = 0.5$, and if for simplicity we put the ratio $\eta'/\eta'' = 1$ because both η's are similar functions of the thrust, then we obtain for the ratio of the time constants

$$\frac{\tau_p}{\tau_w} = 4\pi^2 \cdot 8 \cdot \frac{0.05}{2.5} \cdot 0.5 \cdot (0.2)^2 \cdot 1 = 12.6 \text{ per cent.}$$

Hence the propeller time constant will always be only a small fraction of the water time constant, which we found to be of the order of 1 sec., and thus the water inertia plays a much larger role during reversal than the propeller inertia itself.

If we will compute the backing and reversal periods of the propeller accurately, we must take for the time constant τ in eqs. (36) to (44) the sum of the three time constants for propeller, propeller water, and motor with rotating accessories driving the propeller. Since the time constant of an electric propulsion motor is usually of the order of 1 or 2 sec., the total time constant will be about 3 sec., such as used in our former numerical examples for the retardation time of the propeller. For a geared turbine the time constant usually is much larger. We see that the propeller itself with a time constant of only some tenths of a second plays the least part among the time constants and inertia masses.

If the propeller is driven by an alternating-current electric motor with squirrel-cage winding in the rotor, the entire heat and temperature rise, developed in the squirrel-cage during any transient period of speed,

is directly proportional to the kinetic energy of the rotating masses.[13] Hence the inertia of the propeller water plays a major part in the heating conditions of the driving electric motor, and since the temperature rise constitutes one of the limitations of the maneuverability of the motor, the water inertia is of considerable importance for electric propulsion.

Under any transient or accelerating conditions of the propeller, the difference of the thrust S, produced directly by the motor torque Q, see eq. (49), and the thrust T, resisting by a steady-state action of the water column, see eq. (6), accelerates the inertias of all of the three masses which we have considered, namely, of the motor, propeller, and water. Thus we can subdivide the accelerating force of eq. (34), with respect to the rigid and liquid masses to be accelerated, into

$$S - T = (m_m + m_p)\frac{dU}{dt} + m_w \frac{dU}{dt} \tag{63}$$

where the subscripts m, p, w indicate the motor, propeller, and water masses, the first two being related to the column velocity U, as previously considered in sections 4 and 5. Since the motor thrust S, over the major part of the range, has opposite direction to the propeller thrust T, their absolute difference is taken in eq. (63). In Fig. 27 the former Fig. 18 is repeated, only that in Fig. 27 more details of the

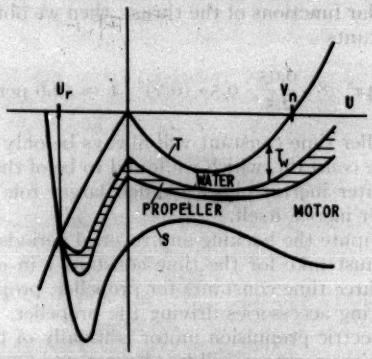

FIG. 27. Subdivision of accelerating forces during reversal of propeller.

decelerating forces are shown. All three inertia masses of eq. (63) are subjected to the same acceleration dU/dt, and therefore the entire thrust difference at any moment has to be subdivided in direct proportion to the masses or to the time constants in order to find separately the three forces decelerating the motor, the propeller proper, and the water surrounding the propeller. For a rigorous determination of the

retardation times of the various masses, one may use simultaneously a U-scale for the liquid parts and an N-scale for the rotating parts. Thus we see that during the transient period the motor torque splits up into three main portions: one gives the steady-state thrust driving the ship, a second accelerates the rigid rotating parts such as motor and propeller, and a third accelerates the liquid parts, namely, the water surrounding the propeller.

The thrust moving the propeller vortex, with its great time constant, constitutes a major part of the entire excess thrust. Moreover, while the moving forces on the rotating masses m_m and m_p are used up by their acceleration or retardation, the accelerating axial thrust on the inertia mass m_w of the water exerts a reaction on the propeller, producing an additional thrust

$$T_w = m_w \frac{dU}{dt} = \frac{m_w}{m_m + m_p + m_w}(S - T) = \frac{\tau_w}{\tau_m + \tau_p + \tau_w}(S - T). \quad (64)$$

The term involving the three masses is obtained by substituting the thrust difference of eq. (63) for the acceleration and in the last term the time constants are substituted for the masses. The magnitude of this thrust can be taken directly from the diagram Fig. 27 by subdivision of the entire excess torque in the ratio of the time constants.

Thus the propeller can develop not only a steady-state thrust by formation of a unidirectionally-ejected water column, but also a transient thrust produced as reaction to the formation and acceleration of a water vortex around the propeller. In the diagram Fig. 27 thrusts T and T_w together constitute the actual force on the propeller during transient conditions. Such a thrust, exerted on the moving ship during the period of backing and of reversal of the propeller, fills up to a considerable degree the deficiency shown in Fig. 17, as is indicated there by the dashed curve.

8. PRESSURE DROP AND CAVITATION.

The conditions of the flow of water in and around the propeller region during backing and reversal are greatly changed as compared with normal operation. Therefore it is useful to investigate the change in pressure of the propeller water, since cavitation possibly may occur during the reversal process. There are now two causes which will develop a pressure drop at the propeller disk, namely, the static forces inherent in the high velocity of the water through the propeller plane, and the dynamic forces of deceleration of the water under transient conditions.

We consider first the transient pressure in the water during retardation of the propeller. The transient vortex of Fig. 24 is symmetrical to both sides of the propeller disk. Therefore the transient thrust,

given by eq. (64) and shown in Fig. 27, is divided into equal parts for the two sides of the propeller, producing a drop and a rise of pressure on opposite sides, each of a magnitude

$$p_d = \pm \frac{1}{2}\frac{T_w}{A} = \pm \frac{\tau_w/2}{\tau_m + \tau_p + \tau_w}\frac{S - T}{A}. \tag{65}$$

Since the propeller during backing and reversal changes the direction of its thrust on the water continuously from astern to ahead, the water will be accelerated at each instant in the ahead direction. Therefore, the retarding propeller always presses on its front side and sucks on its rear side. This is indicated by the arrows on the streamlines in Fig. 24, and thus the positive sign of eq. (65) refers to the front, the negative sign to the rear area of the propeller disk.

During the entire reversal time the rear propeller side thus suffers a transient suction. In Fig. 28 the whole transient force on the inertia of the propelling water is divided into halves and thus the vertically shaded area shows quantitatively the magnitude of the transient suction

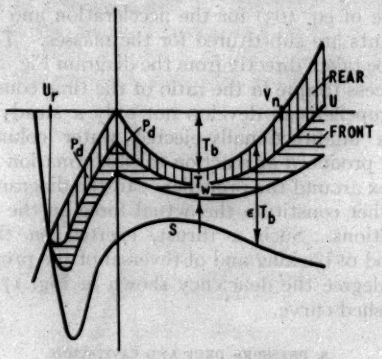

FIG. 28. Subdivision of forces and dynamic pressures at the propeller water during reversal.

thrust on the propeller. We see that three speed zones are particularly affected by high suction, namely, the neighborhoods of full speed ahead; of zero speed; and of reversed speed just under the maximum torque of the driving electric motor.

For a simple survey of the suction effect during reversal of the motor, we can transform the last quotient of eq. (65) into specific terms, and if we now denote by ϵ the ratio of the excess torque of the motor at any speed to the maximum backing thrust T_b, we obtain, with use of eq. (15),

$$\frac{S - T}{A} = \frac{\rho}{k}(\bar{S} - \bar{T}) = \frac{\rho}{k}\epsilon\bar{T}_b = \frac{\rho}{k}\epsilon\frac{V_n^2}{4}. \tag{66}$$

Herein ϵ is a coefficient which usually departs from a value larger than 1 at full speed ahead, shrinks to the torque excess ϵ_b at half speed ahead, increases for the most part to more than 1 at zero speed of the propeller, and reaches again a maximum near full speed astern under the peak torque of the driving electric motor. The suction at the rear propeller side now becomes, substituting eq. (66) in eq. (65).

$$p_d = -\frac{\epsilon}{4} \cdot \frac{\rho}{k} \frac{\tau_w/2}{\tau_{m+p+w}} V_n^2. \tag{67}$$

Thus, if the motor diagram is given, this transient pressure drop always can be determined.

As an example, we compute this value for a ship of $V_n = 20$ kn. $= 10.3$ *m/sec*, a ratio of the time constants τ of 1/3, a density $\rho = 10^3$ *kg/m*^{3}/9.81 *m/sec*^{2}, and an excess coefficient of the motor torque of about $\epsilon = 1.5$ in the more dangerous zones. In order to obtain the limiting value of the suction, occurring with high contraction of the propeller column, we choose here a coefficient $k = 0.5$. Then we obtain

$$-p_d = \frac{1.5}{4} \cdot \frac{10^3}{0.5 \cdot 9.81} \cdot \frac{0.5}{3} \cdot 10.3^2 = 1350 \frac{kg}{m^2} = 0.135 \text{ atm.}$$

This amount is not extremely large; however, the ratio 1/3 of the time constants refers to values for the water of about 1 sec., the propeller of about 0.2 sec., and the motor of about 1.8 sec. If the motor value should be smaller, down to 0.8 sec., the ratio of time constants will approach 1/2 and the suction is increased to 0.203 atm. Furthermore, we must note that this suction refers merely to the mean value over the entire propeller disk, while locally it may become much larger.

In addition to the transient pressure drop at the rear side of the propeller disk, there develops a steady-state hydrostatic pressure drop which is determined by the velocity of the inflow of water to the propeller. According to Bernoulli's theorem, the total pressure heads of the undisturbed water, flowing uniformly with velocity V, and of the inflowing water, entering the propeller with velocity U, are

$$p_V + \frac{\rho}{2} V^2 = p_U + \frac{\rho}{2} U^2, \tag{68}$$

where the subscripts of the static pressures p refer to the corresponding velocities. Thus the static pressure difference between the undisturbed water and the inflow side of the propeller, both at the same depth under the surface, is

$$p_s = p_U - p_V = \frac{\rho}{2}(V^2 - U^2). \tag{69}$$

This hydrostatic pressure drop is independent of the direction of the water flow through the propeller, or of the direction of the ship's

motion. Therefore it applies to all the streamline patterns of Figs. 3–10 or to any transitory change, but always refers to the inflow side of the propeller.

Figure 29 shows the parabolic variation of this inflow pressure with velocity U of the propeller water if the ship's velocity V is kept constant. As long as the propeller is driving the ship with $U > V$, there is suction on the front side of the propeller. The pressure passes through zero if the propelling velocity decreases through the ship's velocity, and becomes positive for backing of the propeller because the inflow velocity, still on the front side of the propeller, now is smaller than the ship's

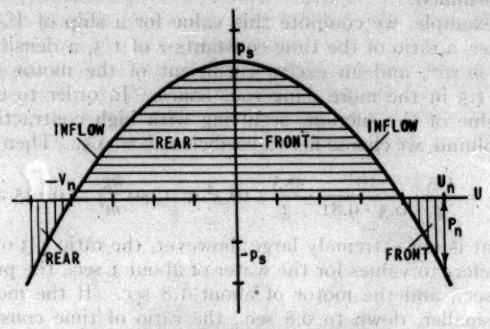

FIG. 29. Static pressure head at inflow side of propeller vs. propeller speed at constant ship velocity.

velocity, see Fig. 7 and eq. (69). The inflow pressure is a maximum at standstill of the propeller water, decreases to zero with reversed water speed of full ship's velocity, and finally changes to suction with further increase of negative propeller speed. However, with reversed propeller the inflow passes over from the front to the rear side of the propeller, as seen in Figs. 9 and 10, and thus the left-hand side of the parabola in Fig. 29 belongs to the rear side of the propeller disk.

At full speed ahead of ship and propeller the normal static inflow pressure drop is, with use of eq. (2),

$$p_n = \frac{\rho}{2}(V_n^2 - U_n^2) = -\frac{\rho}{2} s_n(2 + s_n) V_n^2. \qquad (70)$$

For a slip $s_n = 20$ per cent. and a speed of 20 kn., this gives a suction

$$-p_n = \frac{10^3}{2 \cdot 9.81} 0.2 \cdot (2 + 0.2) \cdot 10.3^2 = 2370 \frac{\text{kg.}}{\text{m.}^2} = 0.237 \text{ atm.}$$

However, it is smaller if the normal slip is less.

If the propeller speed becomes less than the ship's velocity, the inflow side of the propeller obtains static excess pressure because the water is now retarded, as seen in Fig. 29 and explained by Fig. 7. However, in this range the propeller produces a backing thrust directed against the motion of the ship as seen in the lower line of Fig. 11, and thus the pressure on the inflow side is greater than that on the outflow side. Therefore the pressure on the outflow side of the propeller develops as difference between the static pressure on the inflow side, given by eq. (69), and the propeller thrust, givenb y eq. (6) or (9) divided by the area A of the propeller plane. Hence the static pressure on the rear side of the backing propeller is

$$p_s = \frac{\rho}{2}(V^2 - U^2) - \frac{T}{A} = \frac{\rho}{2}(V^2 - U^2) - \frac{\rho}{k}\bar{T}. \qquad (71)$$

Depending upon circumstances this may give either an excess pressure or a suction. If we substitute the velocities for the specific thrust $\bar{T}$, as given by eq. (9), we obtain

$$p_s = \frac{\rho}{2}\left[V^2 - \frac{2}{k}UV + \left(\frac{2}{k} - 1\right)U^2\right]. \qquad (72)$$

Thus also on the rear propeller side the pressure follows a parabola, which is represented over the backing range in Fig. 30.

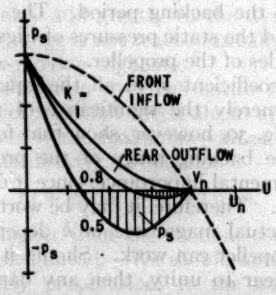

FIG. 30. Static pressure head at outflow side of propeller vs. propeller speed at constant ship velocity.

The magnitude and sign of this pressure are highly dependent on the numerical value of the coefficient of contraction k. Figure 30 shows three curves, for $k = 1$, 0.8, and 0.5. The usual propeller theories assume for k the value 1/2 and this would give the highest suction on the rear propeller side over the largest part of the backing

range. Generally, the minimum of eq. (72) occurs at

$$U = \frac{V}{2\left(1 - \frac{k}{2}\right)} \tag{73}$$

and has the magnitude

$$p_S = \frac{\rho}{2} V^2 \frac{\left(\frac{1}{k} - 1\right)^2}{1 - \frac{2}{k}}. \tag{74}$$

For $V = V_n$ and with $k = 0.8$ this is

$$p_S = -\frac{\rho}{2}\frac{V_n^2}{24}, \tag{75a}$$

with $k = 0.5$, however, the value is much larger

$$p_S = -\frac{\rho}{2}\frac{V_n^2}{3}, \tag{75b}$$

while with $k = 1$ the suction vanishes. In our numerical example, we obtain the limiting value, with $k = 1/2$,

$$-p_S = \frac{10^3}{6 \cdot 9.81} 10.3^2 = 1770 \frac{\text{kg}}{\text{m}^2} = 0.177 \text{ atm}.$$

Hence a considerable static pressure drop may develop at the rear propeller side during the backing period. The transient or dynamic pressure of Fig. 28 and the static pressures of Figs. 29 and 30 superpose on their respective sides of the propeller.

The contraction coefficient k, in all the equations for thrust and backing times, has merely the significance of a multiplying factor. Equation (72) and Fig. 30, however, show that for the development of static pressure in the backing range of the propeller the numerical value of k is of fundamental importance, since it determines whether or not suction will occur. Therefore, it may be worth while to investigate experimentally the actual magnitude of k dependent on the various ranges in which a propeller can work. Should it be found that in the backing range k is near to unity, then any danger of static suction would disappear, as seen from the pressure curves in Fig. 30.

In order to obtain a survey of the excess pressures and the suctions related to the front and rear sides, Table 2 shows in detail the various static and dynamic pressures at both sides of the propeller over the entire range during backing and reversal of the propeller.

We see here as well as by comparison of Fig. 28 with Figs. 29 and 30 that during the normal drive ahead of the propeller in steady-state performance, suction appears only on the front side of the propeller.

When backing is started, by suddenly producing a reversed torque in the motor, there develops a dynamic suction on the rear side of the propeller which soon overcomes the decreasing previous static pressure on that side. This transient suction remains on the rear side of the propeller during the entire period of reversal of the motor and changes in magnitude, as seen by the vertically shaded strip of Fig. 28. In addition to this retardation suction, there may appear on the rear side

TABLE 2.

Development of Pressure Near the Propeller in the Various Regions of Propeller Reversal.

Propeller Region		Static pressure at rear side	Static pressure at front side	Dynamic pressure at rear side	Dynamic pressure at front side
Driving ahead	$U > V$	excess	*suction*	suction	*excess*
Backing	$U < V$	partly suction	*excess*	suction	*excess*
Reversed	$U < 0$	*excess*	high excess	*suction*	excess
Heavily reversed	$U < -V$	*suction*	high excess	*suction*	excess

italic: *inflow side;* standard: outflow side.

of the propeller a steady-state suction during the backing range of the propeller, dependent on the value of the jet contraction. This component changes over to excess pressure, remaining so on both sides of the propeller during the reversed drive, and counteracts the dynamic suction. For extremely large reversed speed of the propeller, however, we may obtain again a static suction, as also seen on the left-hand side of Fig. 29. Here it may add greatly to the dynamic suction on the rear side. This latter range is not reached usually with seagoing ships, but may occur in slow-moving tugboats.

On the whole, the suction over the entire range of backing and reversal of the propeller from full speed ahead appears to develop not too unfavorably. Even if the maximum values, computed for a ship of 20 *kn*, should add up directly, the suction

$$p_d + p_s = -0.312 \text{ atm.}$$

is only 31 per cent. higher than the suction, computed by eq. (70), while traveling full speed ahead. We should notice, however, that the latter suction is nearly proportional to the normal slip, while the backing and reversal suction is independent of this slip. Therefore with propellers of small slip, the suction during the reversal period may exceed considerably the suction during normal drive ahead.

Furthermore, while our calculations refer to the pressure drop or suction covering the propeller disk as a whole, the local vacuum at the propeller blades may be much larger.[10] First, because the thrust corresponding to the pressure is actually developed over the small propeller area a instead of the large disk area A, resulting in an increase

up to the local value $p \cdot A/a$, an effect which may double or triple the magnitude of the suction over the blades; second, because the blades by effect of circulation, viscosity and vortex formation produce local velocity differences adjacent to their edges; third, because the propeller during backing and reversal is working with opposite thrust direction compared to normal operation and therefore produces excess pressure and suction on the hydrodynamically wrong sides of the blades; fourth, because the sharp inversion of the streamlines, between inflow and outflow of the propeller in Figs. 9 and 10, tends to produce a vacuum vortex of its own at the rim of the propeller disk. The first two items are also present at normal propeller operation; the last two, however, are detrimentally present only during the reversal period.

If the actual pressure drop approaches 1 atm. = 10,000 kg/m^2, cavitation occurs and the propeller will lose partly or entirely its hold on the water. Then the production of an effective thrust breaks down and with simultaneously vanishing propeller torque the motor accelerates the propeller rapidly, thereby increasing the causes and effects of the cavitation. Thus the propeller races towards its reversal speed of equilibrium, completely disturbing the regular flow of water about the blades. Only after a lapse of a substantial period of time can a useful water column be built up by the speeding propeller and thus the ship remains without material backing thrust during such interval which is lost for attaining a short headreach and a quick standstill.

The static pressure drop in the backing range, as given by eq. (72), cannot be influenced by the design since all parameters are fixed values for a given ship. Hence it would be advantageous to use an appropriate reversing motor torque from the beginning, reducing any dangerous dynamic suction as given by eq. (67) and entirely avoiding cavitation.

During reversal of the propeller at nearly full velocity of the ship, according to eq. (69) and Fig. 29, the static pressure p_s on the front side of the propeller will practically never attain a negative value. However, if the ship moves slowly, either as a tugboat or near the end of its stopping period, the velocity U of the propeller water may greatly exceed the ship's velocity V. Figure 31 represents various pressure parabolas for lowered ship velocities, and shows that a considerable amount of suction can occur if the negative velocity of the propeller water highly exceeds the ship's velocity.

If, for example, the propeller water is kept at $U_r = -V_n/2$ during backing of the ship and the ship has slowed down to $V = V_n/4$, a suction appears which for our numerical example is

$$p_s = \frac{\rho}{2}\left[\left(\frac{V_n}{4}\right)^2 - \left(\frac{V_n}{2}\right)^2\right] = \frac{10^3}{2 \cdot 9.81}\,\frac{1-4}{16}\,10.3^2$$

$$= -1010\,\frac{\text{kg.}}{\text{m.}^2} = -0.101 \text{ atm.}$$

For standstill of the ship this increases further to − 0.135 atm. However, if the reversed propeller should enforce a higher column velocity of say $U_r = -V_n$ in order to produce a higher backing thrust, the suction at $V = V_n/4$ would be

$$p_s = \frac{10^3}{2 \cdot 9.81} \frac{1 - 16}{16} 10.3^2 = -5060 \frac{\text{kg.}}{\text{m.}^2} = -0.506 \text{ atm.},$$

increasing to − 0.540 atm. at standstill. This is considerably greater and approaches the dangerous values leading to cavitation.

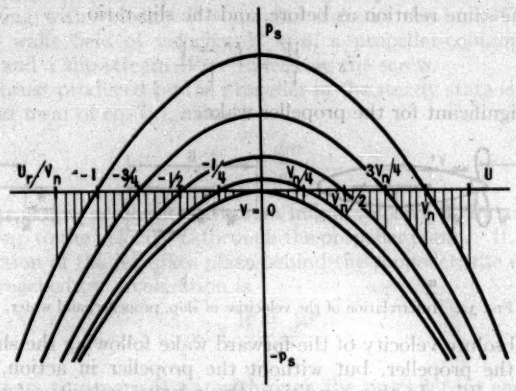

FIG. 31. Static pressure head at inflow side of propeller vs. propeller speed for various ship velocities.

The use of high propeller speed at or near standstill of the ship thus leads more easily to cavitation than at greater velocity of the ship, as is clearly seen from Fig. 31. The reason is that, according to Bernoulli's theorem, the ship velocity V always creates a pressure of motion which is additional to the static atmospheric pressure. Hence it is not advisable to increase the reversed propeller speed too much towards the end of the stopping period or at the beginning of a starting period. Otherwise it might happen that the propeller loses by cavitation its hold on the water and the thrust collapses completely.

APPENDIX 1. INFLUENCE OF THE FORWARD WAKE.

In the main text secondary effects are omitted in order to concentrate the attention on the phenomena of primary importance during reversal. The wake of the hull following the ship is the most significant of the secondary effects and is worthy of additional consideration. Thus we will derive the effect of the resistance wake on the formation

of the thrust during reversal, this wake being produced by the combined action of friction and viscosity, stream line flow and wave formation about the ship.

The various velocities now being considered are shown diagrammatically in Fig. 32a with respect to their location and in Fig. 32b with respect to their quantitative interrelation. The velocities V of the ship, U of the propeller column, and W of the jet are defined in the main text, see eqs. (1) and (2). Thus the propeller wake

$$W = U - V \tag{1}$$

follows the same relation as before, and the slip ratio

$$s = \frac{W}{V} = \frac{U - V}{V} \tag{2}$$

is again significant for the propeller wake.

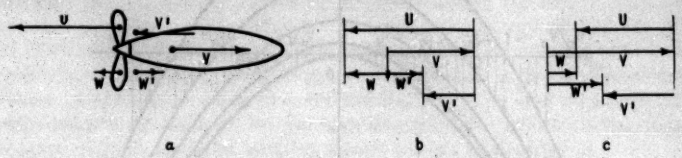

FIG. 32. Interrelation of the velocities of ship, propeller, and water.

The absolute velocity of the forward wake following the ship at the place of the propeller, but without the propeller in action, may be denoted by W'. In this condition, the relative velocity of the water behind the ship is given by

$$V' = V - W'. \tag{76}$$

Thus the propeller, when actually working behind the ship, sucks the water from a field of streamlines of velocity V' smaller than V. Figure 32b shows the interrelation of all the absolute and relative velocities considered. We will designate the ratio of the absolute velocity of the resistance wake to the velocity of the ship by

$$r = \frac{W'}{V}. \tag{77}$$

The propeller moving with the velocity V of the ship accelerates the water approaching the propeller with velocity V' to the higher velocity U, and therefore the total increment of velocity caused by the propeller action will be $W + W'$, as seen in Fig. 32b. Thus the total wake fraction produced by the propeller is

$$s + r = \frac{W + W'}{V}. \tag{78}$$

If in normal operation ahead the propeller should accelerate the water by an amount smaller than the forward wake W' of the hull, the slip-stream W is negative and the diagram of velocities changes to that of Fig. 32c. Now the velocity U of the propeller column is smaller than the velocity V of the ship, and the propeller wake flows in the direction of the travel, as is well known.

By all these kinematic relations the streamline patterns shown in Fig. 3 to Fig. 10 will not be altered in principle. However, the patterns will be related to somewhat different values of the ship velocity. For example, the streamline pattern of Fig. 3 may now correspond to a ship moving with velocity $V = 12$ and wake of the hull $W' = 4$, an inflowing wake field of velocity $V' = 8$, a propeller-column velocity $U = 24$, and a slip-stream $W = 12$ leaving the screw.

The thrust produced by the propeller in the steady state is given by the second term of eq. (3), namely

$$T = v\frac{dm}{dt}. \tag{79}$$

The water is now accelerated from an inflow velocity V' by an amount $W + W'$ up to the velocity U through the propeller plane. If, however, a contraction of the jet takes place behind the propeller, the maximum velocity reached by acceleration is

$$v = \frac{W + W'}{k}. \tag{80}$$

The mass transport of water through the propeller, as enforced by the column velocity U, is

$$\frac{dm}{dt} = \rho A U, \tag{5}$$

as it was before. Thus by eq. (79) the thrust developed by the propeller is

$$T = \frac{\rho}{k} A(W + W')U. \tag{81}$$

According to eqs. (1) and (76), the sum of the wakes is

$$W + W' = U - V' \tag{82}$$

and thus we can express the specific thrust of the propeller as

$$\bar{T} = \frac{T}{\frac{\rho}{k}A} = U(U - V'). \tag{83}$$

We realize that with inclusion of the resistance wake of the hull the propeller thrust is given by a relation of the same character as in eq.

(9) of the main text. However, instead of the velocity V of the ship, there appears here the smaller velocity V' of the forward wake flowing towards the propeller. These two velocities are interrelated according to eqs. (76) and (77) by

$$\frac{V'}{V} = \frac{V - W'}{V} = 1 - r. \tag{84}$$

Since the wake fraction r is assumed usually as a constant of the hull, the velocity V' can be considered always as given and as proportional to the ship velocity V. Hence the thrust-velocity characteristic of the propeller under the influence of the wake of the hull remains a parabola, as shown in Fig. 33. The scale of the parabola, however,

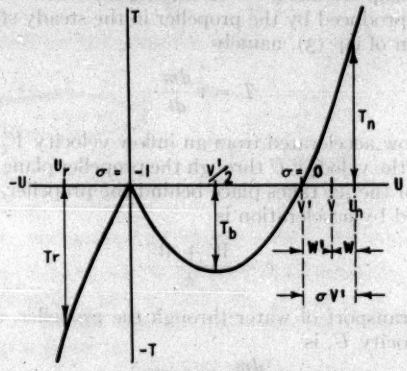

FIG. 33. Propeller thrust under the influence of the resistance wake of the hull.

is reduced as compared to the case with zero wake of the hull. Figure 33 shows also the correlation of the various velocities, namely of propeller column U, ship V, inflow water V' and wakes W of the propeller and W' of the hull.

We now relate the total wake $W + W'$ to the velocity V', rather than to the ship velocity V, and term the quotient

$$\sigma = \frac{W + W'}{V'} \tag{85}$$

the effective slip ratio. Then our problem leads to the same general conclusions as are derived in the main text if only we replace in all the formulas the velocity V by V', the wake W by $W + W'$, and the slip ratio s by σ. Also all the diagrams of the paper remain valid and now will include the influence of the wake of the hull.

At normal velocity U_n of the propeller column, a normal thrust T_n is developed, as shown in Fig. 33. For lower propeller speed, with constant velocities V and V', the thrust driving the ship decreases and passes through zero when the velocity U of the propeller column just coincides with the velocity V' of the inflowing wake. In this case there is no acceleration of water by the propeller, and no thrust will be developed. For still lower propeller speed the thrust becomes negative,

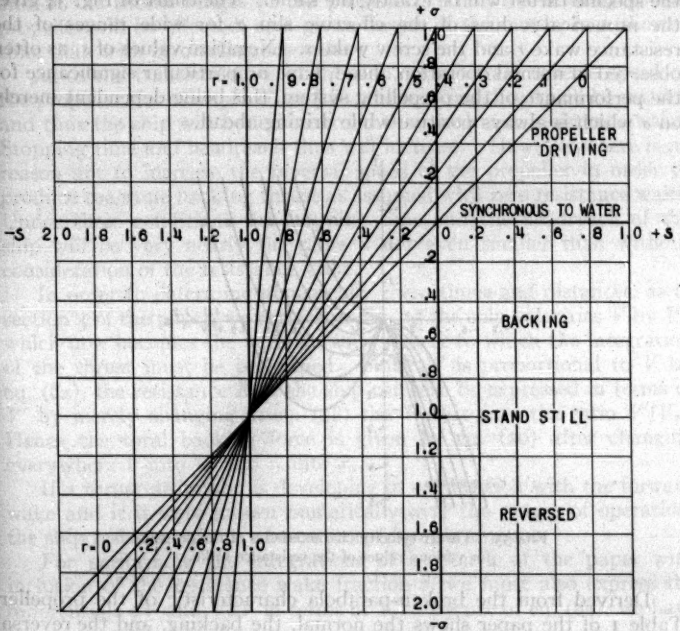
+σ
r = 1.0 .9 .8 .7 .6 .5 .4 .3 .2 .1 0
PROPELLER DRIVING
SYNCHRONOUS TO WATER
−s 2.0 1.8 1.6 1.4 1.2 1.0 .8 .6 .4 .2 0 .2 .4 .6 .8 1.0 +s
BACKING
STAND STILL
REVERSED
r = 0 .2 .4 .6 .8 1.0
−σ

FIG. 34. Effective slip ratio σ against propeller wake fraction s as depending on resistance wake fraction r.

passes through the maximum T_b, and approaches zero for standstill of the propeller. For negative propeller speeds a steeply ascending thrust again develops, shown in Fig. 33 as braking force, as proved in the main text.

The effective slip ratio σ of eq. (85) can be expressed by the wake fractions s and r of eqs. (2) and (77) as

$$\sigma = \frac{W + W'}{V} \frac{V}{V'} = \frac{s + r}{1 - r} \tag{86}$$

wherein eq. (84) also is used. The effective slip ratio σ completely determines the behavior of the propeller behind the ship, as did the slip ratio s for the propeller in open water. Hence, many pairs of values s and r will lead to identical performance of the actual propeller. For example, an effective slip ratio $\sigma = 33.3$ per cent. may result from $r = 0$ and $s = 33.3$ per cent., or from $r = 10$ per cent. and $s = 20$ per cent., or from $r = 40$ per cent. and $s = -20$ per cent. In all three cases the specific thrust will be exactly the same. The chart of Fig. 34 gives the numerical values of the effective slip σ for wide ranges of the resistance wake r and the screw wake s. Negative values of s, as often observed in normal operation ahead, have no particular significance for the performance of the propelling system, this being dependent merely on σ which is always positive while driving ahead.

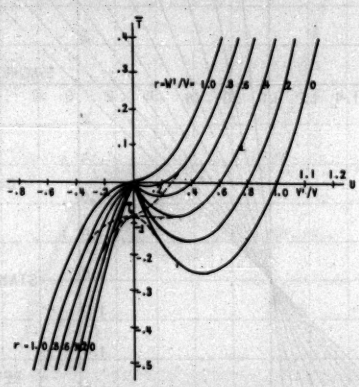

FIG. 35. Thrust-velocity characteristics of the propeller for various values of the resistance wake.

Derived from the broken-parabola characteristic of the propeller, Table I of the paper shows the normal, the backing, and the reversal thrusts, depending on the normal slip s_n of the propeller when driving ahead in open water. We see that this table remains unchanged for the propeller working behind the ship in the wake of the hull, except that now we have to enter the table via the normal effective slip σ_n instead of the normal slip s_n and to relate the thrusts to $V_n'^2$ instead of to V_n^2.

Figure 35 shows an entire family of characteristics giving the correlation of the specific thrust $\bar{T}$ to the velocity U of the propeller column for various values of the wake fraction r as caused by the water resistance of the hull. A forward wake of 40 per cent., for example, displaces the broken parabola so that all the retarding thrusts will be

considerably smaller than with zero wake. In the limiting case of $r = 1$, signifying a resistance wake of equal magnitude with the ship velocity, the two branches of the parabola would become symmetrical and the negative-thrust maximum for propeller speeds ahead would disappear entirely.

Also in the transient state of the propeller, the backing forces of the water are reduced by effect of the resistance wake r both in the ahead and in the astern ranges of the propeller. Thus the reversal of the propeller will be effected, at a given torque of the motor, in a shorter time than with zero resistance wake.

As to the transient state of the ship, at a certain reverse speed of the propeller, for example $U_r = \frac{1}{2}U_n$, the backing thrust will be smaller and thus the ship will be less retarded than with zero resistance wake. Stopping time and headreach thus will increase. However, there is no reason not to increase the reversal speed of the propeller in order to produce the same backing thrust as assumed with zero resistance wake. Under these conditions the stopping time and the headreach of the ship will be very nearly the same if not even smaller than without consideration of the resistance wake.

In order to determine numerically these times and distances, as in section 4 of the paper, we replace in Fig. 15 the ship velocities V by V', which now becomes the variable with respect to which the integration of the thrust must be performed. Since V' is proportional to V by eq. (84), the resistance R of the ship can also be expressed in terms of V' by merely changing in eq. (18) the V-ratio into the ratio V'/V_n'. Hence the total backing force is given by eq. (20) after changing everywhere V into V' and s_n into σ_n.

If a thrust deduction is developing in conjunction with the forward wake and it it were known numerically over the ranges of operation, the ship resistance R may be corrected by this amount.

For performing the integrations of section 4 of the paper with inclusion of the resistance wake fraction r, we must also express the differentials dV and VdV in terms of V'. By use of eq. (84), we have for the stopping time

$$dV = \frac{dV'}{1 - r}, \tag{87}$$

to be used in eq. (23) and the results derived therefrom. For the headreach we have

$$VdV = \frac{V'dV'}{(1 - r)^2}, \tag{88}$$

to be used in eq. (28) and the results derived therefrom.

Thus we have to include the factor $1/(1 - r)$ in the final formulas for the stopping or reversal times of the ship, and the factor $1/(1 - r)^2$

in the final formulas for the headreach. This will give an increase in the numerical values. However, the integrals themselves taken only up to the smaller upper limit V_w', give a lower numerical value. Hence numerically the entire result will be only slightly different from that derived with omission of the resistance wake. For any actual ship of known resistance wake the evaluation of the integrals, or of the end formulas given in the main text, is in no way more cumbersome than with zero resistance wake.

The thrust T_0 at zero speed of the propeller must be considered separately. If the propeller moves without rotation through water of the velocity V', as given by eq. (76), the drag is proportional to V'^2 rather than to V^2, as in eq. (10). Hence the filling up of the zero depression in the curve as shown in Fig. 14, follows a conversion in scale similar to that of the entire thrust characteristic.

The broken parabolas in Fig. 35, with their zero values for standstill propeller, become less extreme in curvature with increasing resistance wake. A certain drag T_0, therefore, will change the shape of the characteristic in a somewhat different way for high or for low resistance wake. This is shown for three examples by the dashed lines in Fig. 35. Hence, high resistance wake r, particularly in combination with large relative blade area of the propeller, a/A, will considerably distort the broken-parabola shape of the characteristic and may more or less smooth out the deep depression at standstill of the propeller. This is sometimes observed in the case of high-speed ships.[16–19,24–26]

Since eq. (83) for the thrust is linear in V', and eq. (76) for V' is linear in W', which is the absolute velocity of the resistance wake, any variation of this velocity W' with time or in space, caused by the irregularity of the hull and by the vorticity of the water, will have a linear influence on the thrust. Hence, we are permitted to use the arithmetic-mean value of the forward wake over the propeller disk for arriving at the actual value of the thrust. For every ship this effective resistance wake can be determined by a test run with zero thrust of the propeller, and is very near to the velocity of the free rotating propeller. If, on the other hand, the impressed velocity U of the propeller column should suffer any variation, the effect cannot be described in a way of similar simplicity, since U enters eq. (83) quadratically.

Sections 5, 6 and 7 of the paper do not deal with phenomena directly dependent on the resistance wake.

In section 8, however, the pressure drop in the propeller water will experience some alteration. Taking the resistance wake into consideration, the numerical values of the backing thrust T_b in Fig. 28 will be reduced and thus for a given torque S of the motor the torque excess ϵ will be augmented. Hence, the accelerating forces on the water and thus the dynamic pressures, excess as well as suction, will be increased.

The static pressure-drop based on Bernoulli's law, also will alter under the effect of the resistance wake, since the basic velocity of the undisturbed water in eq. (68) is only V' rather than V. However, since the propeller speed U also will be smaller and the effective slip σ_n actually will have about the same value which the slip s_n had formerly, the numerical values of the suction will not alter much. With any change of the propeller speed U or the ship velocity V the pressure head will follow the same parabolas as in Figs. 29 to 31, except that V again is to be replaced by V'.

APPENDIX 2. CONTRACTION OF THE PROPELLER WAKE.

The contraction of the jet expelled from the propeller plays an important part in the production of the thrust. This can be seen by eq. (6) where the coefficient of contraction constitutes a divisor to

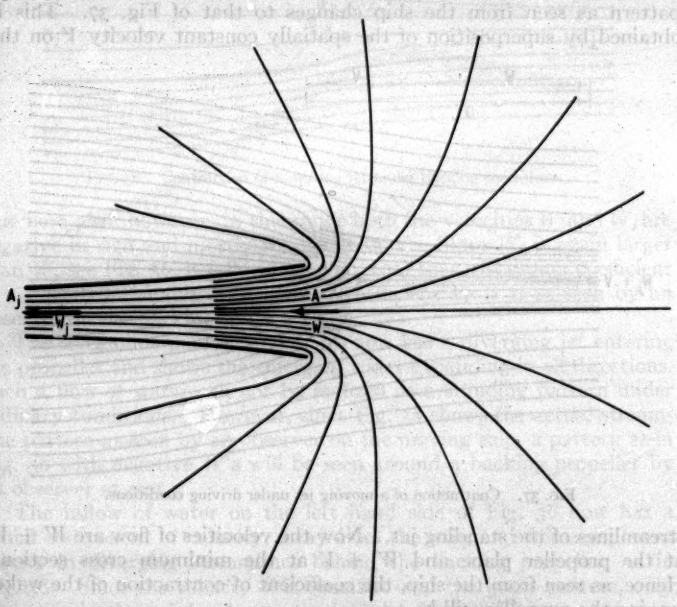

FIG. 36. Contraction of a stationary water jet behind the standing propeller.

which the thrust is inversely proportional. At the present state of knowledge the actual value of this coefficient must be determined experimentally over the entire region of driving, backing and reversing of the propeller. However, it is possible to reach by analysis alone

some general points of view concerning the behavior of the jet contraction over these ranges.

The contraction coefficient of the standing jet is given, as shown in Fig. 36, by the ratio of the areas of propeller disc, A, and minimum cross section, A_j, of the jet behind the propeller. In view of the continuity of the flow of water this ratio determines the ratio of the corresponding velocities of flow through these areas. Thus the coefficient of contraction is

$$k = \frac{A_j}{A} = \frac{W}{W_j}, \tag{89}$$

wherein the subscript j signifies values at the minimum cross section of the jet.

If propeller and jet are moving ahead with velocity V, the streamline pattern as seen from the ship changes to that of Fig. 37. This is obtained by superposition of the spatially constant velocity V on the

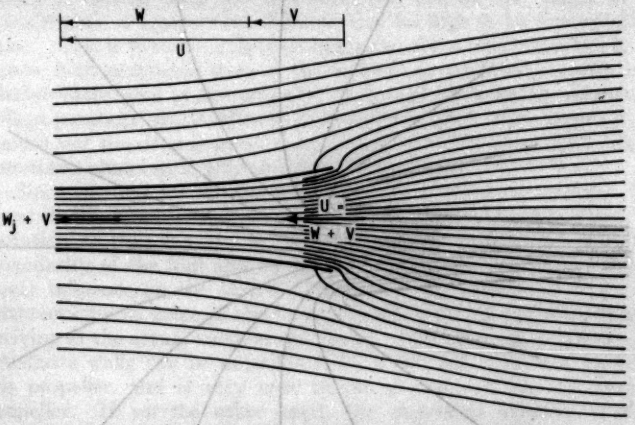

FIG. 37. Contraction of a moving jet under driving conditions.

streamlines of the standing jet. Now the velocities of flow are $W + V$ at the propeller plane and $W_j + V$ at the minimum cross section. Hence, as seen from the ship, the coefficient of contraction of the wake leaving the propeller will be

$$k_V = \frac{W + V}{W_j + V}. \tag{90}$$

For velocities of positive sign, this value is nearer to unity than that of eq. (89) for the standing jet. This is due to the entirely different

pattern of streamlines obtained from the superposition. Only in case the standing jet should experience no contraction would the coefficient be unity for both the standing and the moving jet.

Under backing conditions of the propeller, the absolute water velocity W through the propeller disc is in the direction of travel, see Fig. 11 of the main text. Figure 38 shows for this condition the streamlines with superposed ship velocity V. The general eq. (90) is

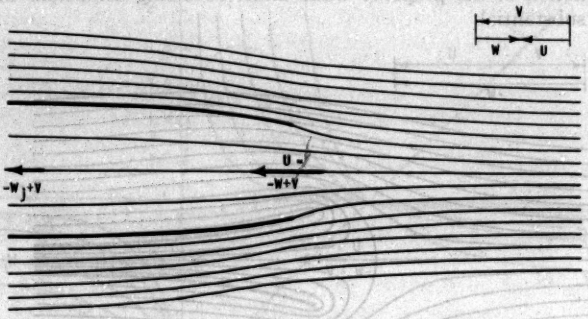

FIG. 38. Contraction of a moving jet under backing conditions.

true here also; however, in this range both the velocities W and W_j are negative in sign and mostly smaller than V. Since W_j is again larger than W, see Fig. 36, it follows from eq. (90) that a standing coefficient $k < 1$ leads inevitably to a moving coefficient $k_V > 1$, as seen by an observer on the backing ship.

The streamline pattern of Fig. 36 now has a diverging jet entering the propeller and shows the emerging water expanding in all directions. Such a flow of water can not be realized as a standing pattern under ordinary conditions. However, since Fig. 38 shows the actual streamline pattern as seen by an observer on the moving ship, a pattern as in Fig. 36 with negative W's will be seen around a backing propeller by an observer at rest.

The inflow of water on the left hand side of Fig. 36 now has a radial component of velocity, away from the axis, and this component results in diverging streamlines behind the backing propeller, as in Fig. 38. Since the velocity V is constant over the whole pattern, only a change in the axial velocity as given by W and W_j can produce a thrust, and this change is represented in the purest form by a standing streamline pattern as in Fig. 36, the velocities being either positive or negative.

Under reversing conditions, both the wake velocity W and the column velocity U of the propeller are negative, as seen by Fig. 11.

Thus the pattern of the standing streamlines again will be the same as in Fig. 36, except that it is reversed in space. The superposition of the constant ship velocity V, now in the opposite direction to W, results in the moving streamline pattern of Fig. 39, and again eq. (90) is true. Since W_j is always larger than W and in this range both wakes of negative sign are larger than V, the contraction coefficient k_V of the moving jet will be smaller than k of the standing jet. Hence the contraction of the propeller wake under reversing conditions may be very substantial.

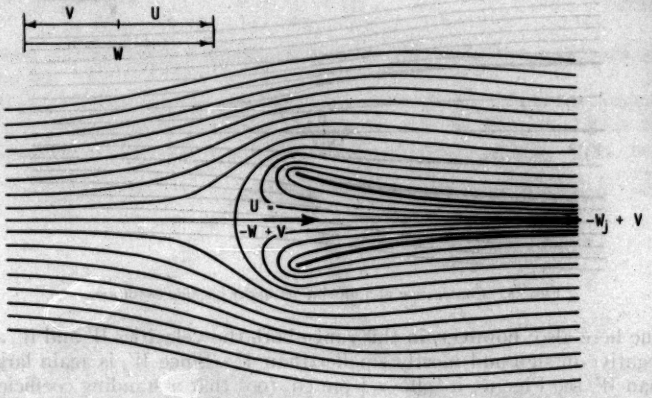

FIG. 39. Contraction of a moving jet under reversal conditions.

The complete reversal of the direction of the streamlines in Fig. 39 between inflow and outflow of the propeller gives this pattern the appearance of a marked vortex system. However, there is only a quantitative difference in the vortex formation of Fig. 39 and that of Figs. 37 or 38, the boundary of the jet always constituting the core of a vortex system.

Figures 36 to 39 indicate that the boundary of the jet will change in space as the constant velocity V is superposed. This displacement of the boundary is the underlying reason for the difference between k_V and k.* In reality, however, the boundary of a jet moving in open water is an unstable surface which moves strongly itself and continuously decays into a more or less regular system of vortices. Thus, under actual conditions, it will be difficult to determine the surface of the jet, and therefore to determine the area of its smallest cross section, since the boundary is so uncertain and so fluctuating. This

* Actually, the boundary of the propeller jet and the core of the vortex system surrounding the jet need not remain identical during superposition. For the sake of simplicity the difference is not considered in Figs. 36 to 39.

uncertainty begins at the propeller plane. Hence the areas A and A_j in eq. (89), and therefore the definitions of the two coefficients of contraction in eqs. (89) and (90) can be related only to an average boundary of the jet as determining the main flow of water through the propeller. A more detailed description of the performance of such a jet must wait for the development of a vortex theory of the contracting jet.

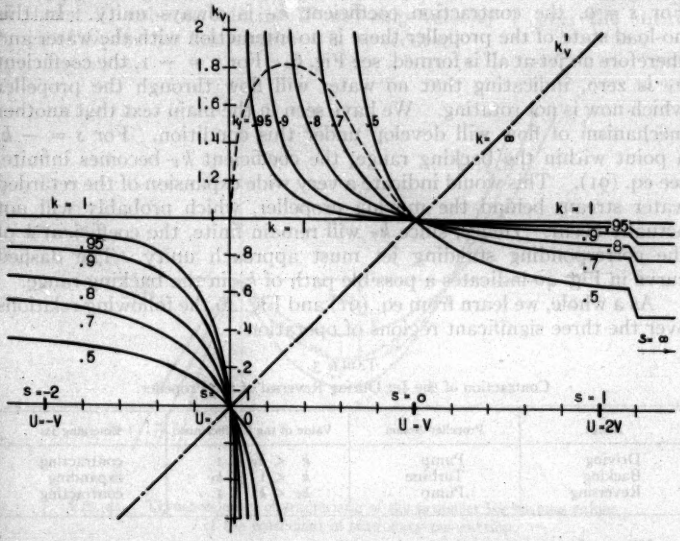

FIG. 40. Contraction of the moving jet versus slip ratio s for various values of the coefficient k of stationary contraction.

Introducing the slip ratio of the propeller wake as defined in the main text,

$$s = \frac{W}{V} \tag{2}$$

into eq. (90), we can express the coefficient of contraction behind the moving propeller as

$$k_V = \frac{1 + \dfrac{V}{W}}{\dfrac{W_j}{W} + \dfrac{V}{W}} = \frac{1 + s}{1 + \dfrac{s}{k}} \tag{91}$$

Hence the contraction of the moving jet depends merely on that of the standing jet, determined by k, and on the slip ratio s. Figure 40 shows

the variation of k_V over the three ranges of driving ahead, backing and reversing, for given values of the coefficient of the standing jet from $k = 0.5$ to $k = 1$. . Compared to the standing flow, the wake behind the moving propeller will contract to a lesser degree in the driving state; it will expand in the backing range and will contract to a greater degree under reversing conditions.

There are three singular points in Fig. 40 worthy of discussion. For $s = 0$, the contraction coefficient k_V is always unity. In this no-load state of the propeller there is no interaction with the water and therefore no jet at all is formed, see Fig. 6. For $s = -1$, the coefficient k_V is zero, indicating that no water will flow through the propeller which now is not rotating. We have seen in the main text that another mechanism of flow will develop under this condition. For $s = -k$, a point within the backing range, the coefficient k_V becomes infinite, see eq. (91). This would indicate a very wide expansion of the retarded water stream behind the moving propeller, which probably will not actually occur. Hence, since k_V will remain finite, the coefficient k of the corresponding standing jet must approach unity. The dashed curve in Fig. 40 indicates a possible path of k_V in the backing range.

As a whole, we learn from eq. (91) and Fig. 40 the following relations over the three significant regions of operation:

TABLE 3.
Contraction of the Jet During Reversal of the Propeller.

Range	Propeller Action	Value of the Coefficients	Emerging Jet
Driving	Pump	$k < k_V < 1$	contracting
Backing	Turbine	$k < 1 < k_V$	expanding
Reversing	Pump	$k_V < k < 1$	contracting

Hence from our analysis there always results such a performance of the moving jet as actually occurs according to common observation. In the usual propeller theories the presumption is that $k = \frac{1}{2}$ throughout. It is evident that with this presumption substantial discrepancies must appear within the backing range. These are well known and until now could not be cleared up.

Since k is determinative for the formation of the thrust, see eq. (6), any variation of k is of high significance for the development of the true thrust-velocity characteristic. Figure 41 shows three parabolic characteristics for values of $k = 0.5$, 0.7, and 1, all other conditions being kept constant. The actual thrust produced by the propeller mechanism probably will remain within the regions indicated by these curves. In the backing range this thrust will start at the origin on the curve with $k = 1$ and near velocity V will approach a curve with smaller k, as indicated by the dashed line which corresponds to the dashed curve in Fig. 40. By this behavior the maximum backing

thrust will be displaced to a column velocity U larger than $V/2$, thus distorting the parabolic shape into the actual characteristic.

For the driving and reversing ranges of the thrust characteristic it is not possible to derive from merely phenomenological considerations as the preceding similar statements concerning the displacement of the actual curve. Since the influence of k on the formation of the thrust is very substantial, it is to be hoped that by simultaneous measurements of thrust T, column velocity U and ship velocity V over the entire range of U, further information will be secured.

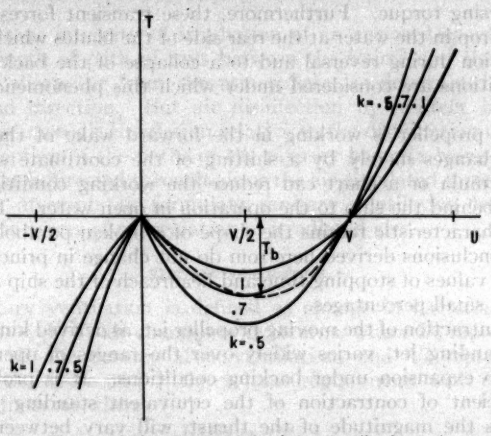

FIG. 41. Thrust-velocity characteristic of the propeller for various values of the coefficient of stationary contraction.

The derivation of eqs. (90) and (91) is merely kinematic and thus we may apply these results also to the inflow side of the propeller water. We see by Fig. 2 that the contraction of the standing streamlines from infinity to the propeller disk corresponds to $k = \infty$, as related to the propeller area. Thus the contraction coefficient of the inflow water, as seen by an observer on the ship is, according to eq. (91),

$$k_V' = 1 + s. \tag{92}$$

This is plotted as a dash-dot line in Fig. 40. For a slip ratio $s = 200$ per cent., there is $k_V' = 3$, which is in accord with the inflow contraction of the streamlines in Fig. 3. For $s = 25$ per cent., we obtain $k_V' = 1.25$ in accord with Fig. 5; for $s = -50$ per cent., we have $k_V' = 0.5$ in accord with Fig. 7; and for $s = -200$ per cent., there develops $k_V' = -1$ in accord with Fig. 9; all these diagrams referring to Part I. In the last example the minus sign of k_V' indicates a change

of direction of the propeller wake with respect to the direction of the inflowing water.

SUMMARY OF PART II.

A consideration of the transient behavior of the propeller exhibits the production of a propeller vortex in the water during every rapid change of propeller speed. This leads to the development of inertia forces due to the mass of the active water surrounding the propeller. These forces add to the inertia forces of propeller and driving machinery in the reversal condition and consume a considerable part of the available reversing torque. Furthermore, these transient forces develop a pressure drop in the water at the rear side of the blades which may lead to cavitation during reversal and to a collapse of the backing thrust. The conditions are considered under which this phenomenon may be avoided.

If the propeller is working in the forward wake of the hull, the analysis changes merely by a shifting of the coordinate system. A simple formula or a chart can reduce the working conditions of the propeller behind the ship to the operation in open water. The thrust-velocity characteristic retains the shape of a broken parabola, and the general conclusions derived herefrom do not change in principle. The numerical values of stopping time and headreach of the ship are altered merely by small percentages.

The contraction of the moving propeller jet, as derived kinematically from a standing jet, varies widely over the ranges of operation and changes to expansion under backing conditions. It is probable that the coefficient of contraction of the equivalent standing jet, which determines the magnitude of the thrust, will vary between one half and unity over the ranges of driving, backing, and reversal of the propeller, thus distorting the parabolic shape of the thrust-velocity characteristic.

CIRCULATION IN SANITARY VENTILATION BY BACTERICIDAL IRRADIATION OF AIR.

BY

W. F. WELLS,

Associate Professor of Research in Air-borne Infection, Laboratories for the Study of Air-borne Infection,* University of Pennsylvania School of Medicine, Philadelphia, Pa.

The average intensity of irradiation of an enclosed space depends upon the length of path of rays between the source and the point at which they disappear from the atmosphere, as determined by their position and direction. But air disinfection by indirect irradiation depends also upon air circulation relative to the distribution of irradiation, interception of the paths of the rays by bacteria being the same whether light is directed through air or the air circulated through light.[1] This paper attempts to formulate sanitary ventilation by indirect irradiation in terms of recirculation of irradiated air.

SANITARY VENTILATION.

If sanitary ventilation is defined as change in bacterial density, D/D_0, by $A = V/V_0$ air changes or overturns, where D_0 represents the initial and D the density after ventilation, and V_0 represents the volume of the space and V the volume replacement with continuous mixing by fresh air, then

$$D/D_0 = e^{-A}.$$

And where lethes of disinfection, L, become the sanitary equivalent of air changes of ventilation,[2]

$$D/D_0 = e^{-L}.$$

Thus LV_0 (cubic foot lethes) is the sanitary equivalent of AV_0 (cubic feet) of ventilation.

The number of killed bacteria—being proportional to the lethal energy intercepted by the living organisms—is a maximum when exposure of living organisms to the irradiation is uniform; and the number of cubic foot lethes of disinfection is proportional to the foot watt minutes (*fwm*) of irradiation,[3] as

$$LV = \alpha fwm.$$

Cubic foot lethes of disinfection then define foot watt minutes of uniform irradiation.

* Subsidized by a grant from the Commonwealth Fund.

RECIRCULATION OF IRRADIATED AIR.

From this reciprocal relation between air volume, V, and lethal exposure, L, it is possible to formulate irradiation of recirculated air. If $V/V_0(=A)$ overturns of recirculated air are uniformly exposed to irradiation, L_0V_0, the fraction of survivors in volume V becomes $e^{-L_0V_0/V}(=e^{-L_0/A})$ and equivalent air changes by fresh air would be $A(1-e^{-L_0/A})$.

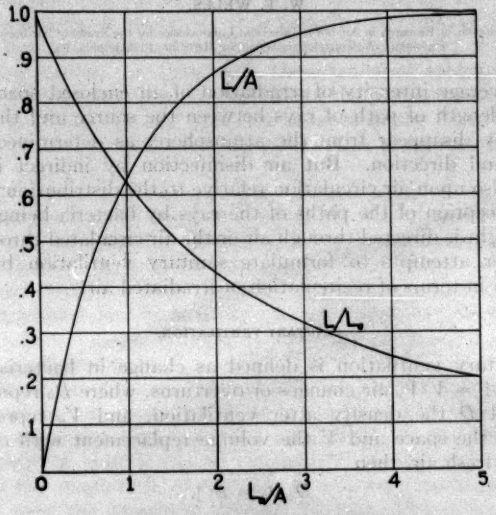

CHART I. Equivalent recirculation of irradiated air.

L—negative natural logarithm of fraction of survivors in room.

L_0—500 times product of mean ray length in feet, lethal flux in watts, and time in minutes; divided by room volume in cubic feet.

A—equivalent recirculation through uniform irradiation (L_0 times volume of room in cubic feet) in air changes or overturns per minute.

The relation between the lethal change by uniform irradiation of a room, as compared to the uniform irradiation of the recirculated air, becomes

$$L/A = 1 - e^{-L_0/A},$$

or

$$-L_0/A = \log_e(1 - L/A).$$

Values of L_0/A, L/A and L/L_0, plotted on Chart I, show that as irradiation relative to recirculation increases, sanitary ventilation, L, approaches recirculation, A; and conversely as recirculation increases relative to irradiation, sanitary ventilation approaches disinfection by

uniformly distributed irradiation, L_0V_0, in the room, V_0. In the limit, sanitary ventilation by infinitely rapid recirculation ($A = \infty$), of uniformly irradiated air, exactly equals disinfection by uniform distribution of irradiation in the room, or $L = L_0$; passage of light through air being the exact equivalent of passing air through light.

In view of the low cost of irradiation compared to recirculation, it is good practice to increase L_0V_0 until the term $e^{-L_0/A}$ nearly vanishes; and L approaches A. The point of diminishing returns is reached at about 99 per cent. disinfection—or about five times the uniformly distributed lethal irradiation required to accomplish equal disinfection in the room.

Irradiation of recirculated air is far more economical than ventilation by fresh air, even though five times the uniform irradiation in a room is required for the same sanitary ventilation. Practical considerations limit recirculation of irradiated air; but the erythemal tolerance of occupants also limits to a similar degree lethal exposure to direct irradiation. The attainable ventilation equivalent of about ten air changes per hour does not suffice to prevent the epidemic spread of air-borne infections during the winter.

CIRCULATION AND INDIRECT IRRADIATION.

This dilemma—controlling air-borne infection by exceeding the limits of practical recirculation or average erythemal exposure—is met by indirect irradiation. If unoccupied regions of a room are flooded with lethal light, the natural circulation of air from the irradiated zones then provides equivalent sanitary ventilation far in excess of that practically attainable in the limiting case by mechanical recirculation.

The spatial distribution of indirect irradiation relative to air circulation is a more general concept than the irradiation of recirculated air. Since, however, the passage of light through air is the bactericidal equivalent of circulating air through light, this abstract concept of sanitary ventilation by radiant disinfection can be expressed as equivalent recirculation of uniformly irradiated air. If L is measured by bacteriologic methods, and L_0 computed from irradiation, $\alpha fwm/V_0$, the value of A can then be derived from L_0/A corresponding to L/L_0 (Chart I).

LETHAL DOSE.

Thus the lethal equivalent of irradiation, or the value of α for uniform irradiation is the key to a study of circulation in the radiant disinfection of air. The lethal equivalent of monochromatic light against *E. coli* in aqueous suspensions and on moist agar surfaces has been established by elaborate studies.[4] A carefully weighted mean gives .027 watt minutes per square foot as the unit of lethal exposure to the 2537 Å resonance band of mercury. But the vulnerability of *E. coli* atomized

into air was found to be of a higher order of magnitude than when suspended in drinking water, and in dry air to be greater than in moist air.[5] The magnitude of this humidity factor, computed from Whisler's experiments,[6] is shown on Chart II. Unfortunately he did not measure light intensities, but the value of a lethal dose of 2537 Å radiation in dry air has been estimated from the rated performance of the standard lamp, within the precision of experimental data, to be .0006 watt minutes per square foot[7].

Since intensity varies inversely as the square of the distance from a source, the uniform irradiation of agar surfaces or small liquid volumes

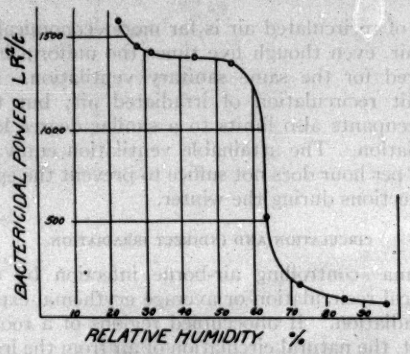

CHART II. Relative lethal power (LR^2/t) of Uviarc against *E. coli* suspended in air of different relative humidities. (Computed from Whisler's data.)[6]

R—distance in feet from lamp.
t—time in minutes.

is much simpler than uniform irradiation of large volumes; and uniform exposure of air suspended organisms becomes extremely difficult. If air could flow freely toward a light source from all directions, the velocity of approach would vary with intensity; and the exposure of air-borne bacteria in passing equal radial distances would be equal. This principle has been applied in an attempt to derive a more precise evaluation of a lethal dose in air (Chart III).

A room twelve feet square was divided into an upper and lower chamber by a seven-foot ceiling. The lower chamber was converted into an octagon by corner partitions between the floor and the ceiling. To simulate further a spherical sector, truncated conical surfaces with apices at the center of the chamber were attached to the ceiling and floor. The truncated ends of the cones served as exhaust outlets through which the air was conducted from the room by ducts. The light source was fixed at the center of the room between these two exhaust outlets.

A fan blower delivered 200 cubic feet of air per minute to the upper chamber, where a diluted culture of *E. coli* atomized into the air stream of the fan exhaust became uniformly distributed and stabilized by the few minutes detention period. Passing down behind the partitions through openings in the corners of the false ceiling, the air emerged in tangential films through narrow slits formed between the left hand edge of the partition and the walls of the exposure chamber. Spiralling toward the central outlets, the velocity of approach remained proportional to irradiation intensity, thus tending to equalize exposure at different radial distances from the light.

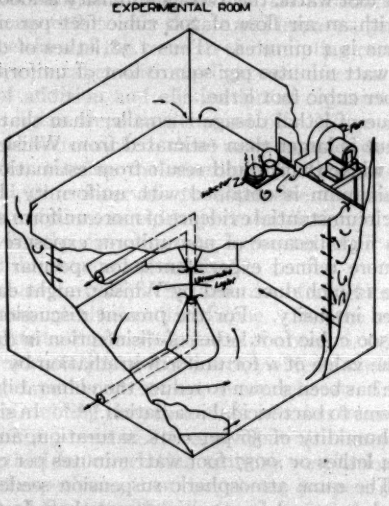

CHART III. Experimental room for measuring lethal equivalent of radiation against air-borne bacteria.

The walls subtended at the light a solid angle of 6.3 steradians, with an average radial distance of 6.6 feet. The ceiling and floor beyond the cones subtended a solid angle of 4.5 steradians, with an average radial distance of 5.0 feet. Thus irradiation from a point source at the center would equal 64 times the radiant flux density per steradian. An unshielded length of a Hanovia Safe-t-aire quartz tube, fixed between the outlets, approximated a point source at the center of the chamber. The average flux density in the solid angle subtended by the ceiling and floor was four-fifths that subtended by the walls, giving weighed total irradiation of 60 times the radiant flux density per steradian in a horizontal direction. The intensity at three feet in a horizontal direction

was determined by a Rentschler photometer to be .00097 watts per square foot, or .00873 watts per steradian, giving a total of .521 foot watts of irradiation in the chamber.

In 20 experiments with an average relative humidity of 33 per cent. saturation, an average bacterial density change of 1.38 lethes was obtained at the exhaust when the light was turned on. Thus .521 foot watts of irradiation yielded 276 cubic foot lethes of disinfection per minute, or .0019 foot watt minutes per cubic foot lethe as a lethal dose in dry air. The lethal dosage can also be computed from time and intensity of exposure. In a chamber of 800 cubic feet capacity, irradiated by .521 foot watts, the average intensity is .00065 watts per square foot, and with an air flow of 200 cubic feet per minute, the average exposure time is 4 minutes. Thus 1.38 lethes of disinfection resulted from .0026 watt minutes per square foot of uniform exposure or .0019 foot watts per cubic foot lethe.

This value of lethal dosage is smaller than that derived by several observers, but is larger than estimated from Whisler's data. The discrepancy is wider than would result from estimation of radiation; and since the minimum is obtained with uniformity, lower values are in themselves circumstantial evidence of more uniform exposure. Whether our value is high because of non-uniform exposure can only be determined by more refined experiments, for specular reflection from the inside of the 12-inch duct used by Whisler might easily have increased the estimated intensity. For the present discussion of circulation, we shall adopt 500 cubic foot lethes of disinfection in dry air per foot-watt minute as the value of α for uniform irradiation by 2537 Å wave band.

Moisture has been shown to reduce the vulnerability of air-suspended microorganisms to bactericidal irradiation.[2, 5, 6] In six experiments, with an average humidity of 56 per cent. saturation, an average lethal exposure of .44 lethes or .0057 foot watt minutes per cubic foot lethe was obtained. The same atmospheric suspension seeded on agar plates—simultaneously exposed for 30 minutes at three feet distance from the light, that is, to .0029 watt minutes per square foot—gave in 34 experiments an average of 1.34 lethes, or .0217 watt minutes per square foot as a lethal dose to *E. coli* on moist agar surfaces. This result compares favorably with the weighted mean of .0273 watt minutes per square foot obtained on moist surfaces and in aqueous suspensions by other investigators referred to above. Obviously the vulnerability of *E. coli* suspended in dry air is of a higher order of magnitude than in aqueous suspension; or on agar surfaces; or in moist atmospheres.

LETHAL EXPOSURE.

The lethal exposure, L, of organisms circulating between points in an irradiated room can also be measured bacteriologically, by atomizing into an atmosphere a standard suspension of test organisms at a constant

rate and determining the bacterial density change, L_a, at another point with the lights off and on. Actually the value of L varies with every location of infector and infectee, and the value of L_a between two arbitrarily chosen points can serve only as a statistical parameter of an infinite number of values. The location of infector and infectee must be carefully selected if the measurement of lethal exposure is to represent sanitary ventilation by indirect irradiation.

In early studies of school rooms, an atomizer was located three-quarters of the distance from the center to a corner of the room; and an air centrifuge was located in a similar position in an adjacent corner. A small household fan blew an air stream over the atomizer, parallel to the diagonal of the long wall, to mix the air and impart a gentle circulation around the three sides of the room to the sampling corner. Three consecutive samples were taken with the lights on, after an equilibrium between the rates of addition and elimination of organisms had been established and the lights were then turned off. When equilibrium, with the lights off had been reached, three more samples were collected; and immediately after turning the atomizer off, three more samples were taken at equal time intervals to determine the dieaway rate. Sanitary ventilation in lethes, or equivalent ventilation in air changes, is given by multiplying the die-away rate, expressed as air changes, by the ratio of the equilibrium concentrations.[8]

Naturally the values vary with the direction of air circulation from infector to infectee through the irradiated zone. Yet the average of 16 tests in centrally lighted square classrooms, of about 6,000 cubic feet, irradiated with approximately four foot watts, yielded a sanitary equivalent of 69 air changes per hour—or approximately 10 times normal winter ventilation. Doubling the amount of radiation from each fixture increased the average of 9 tests to 116 equivalent air changes per hour. The value of the method for correlating sanitary ventilation by air disinfection with clinical experience, then the primary purpose of the study, was demonstrated; and the potential elimination of air-borne infection during the winter by disinfection rates comparable to summer ventilation, when respiratory diseases decline, was established.

In the third experimental year, when supplementary irradiation required retesting, an attempt was made to compensate for directional circulation. With the infector and infectee on a diagonal about half way from the center to opposite corners of the room, tests were duplicated in reversed positions. A general average of 142 lethes, or equivalent air changes per hour, were obtained from 17 such double tests in the different rooms. The fact that an average of the larger in each pair of values was four times the average of the smaller indicated the need of further study of disinfection gradients between various points in the room before devising a more stable method of evaluating the performance of fixture designs.

LETHAL GRADIENTS.

The schoolrooms described in the previous paper [1] provided facilities for studying disinfection gradients in sanitary ventilation. Simultaneous samples were taken in the different corners of a rectangular room with end wall fixtures, the lethal exposures in a series of 17 experiments being averaged on Chart IV (upper). As the air circulated from

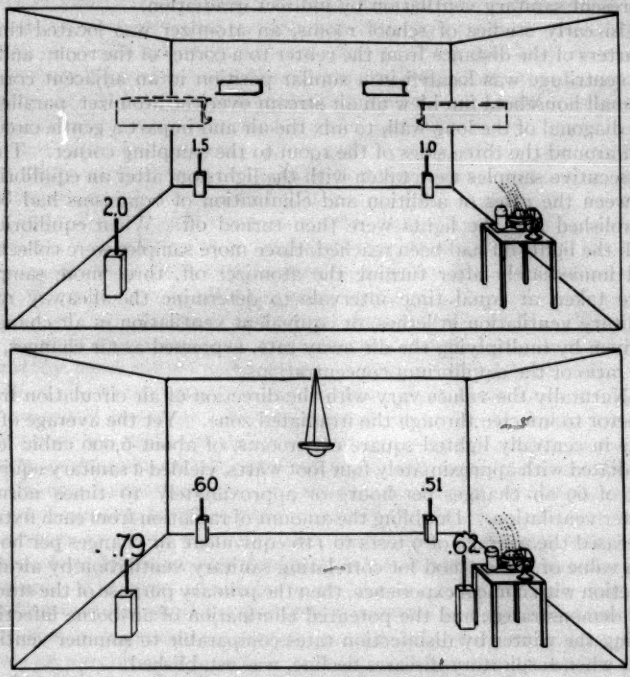

CHART IV. Lethal exposure of organisms atomized into one corner, and sampled at other corners of irradiated classroom.
Upper: Rectangular room (33′ × 22′ × 11′) with end wall fixtures (high beam angle).
Lower: Square room (27′ × 22′ × 11′) with central hanging fixture.

the infector around the room the gradient increased progressively, being in the third sampling corner about double what it was in the first. In the average of 12 runs in the centrally lighted square room (Chart IV, lower) the effect was less pronounced; probably because the gradient depended more upon dilution with the irradiated atmosphere from the core of the room, rather than because of direct circulation through the irradiation. Local mixing might also be indicated by the lower value

obtained in the corner near the infector. The value obtained in the corner opposite the infector approximated the average in the first and third corner in both sets of experiments. Since this more representative test of average disinfection was about three-quarters of that obtained by the method used in the original experiments, the average results can readily be converted.

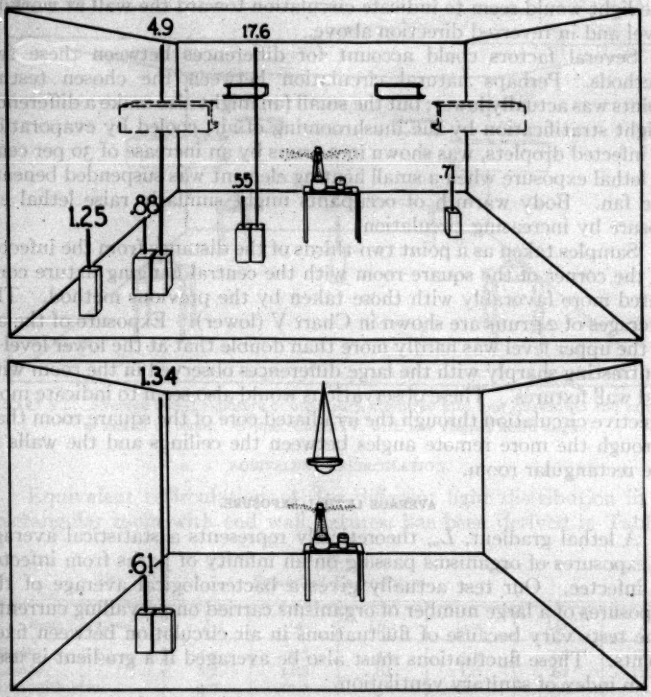

CHART V. Lethal exposure of organisms atomized into center, and sampled at different distances and elevations of rooms shown in Chart IV.

In a second series of experiments, with the infector located in the center of the room, a small fan blower, with housing removed and supported on a tripod above the atomizer, was used to distribute the infected air in a horizontal direction. Samples were collected one-third, two-thirds and five-sixths of the distance from the center, at the middle of the long side, and also one foot below the ceiling at the first two stations.

The average lethal exposures from 81 runs in the rectangular room, shown on Chart V (upper), are considerably lower than in the first series; but increase progressively at working level with distance from the infector. Organisms collected from the upper air of the rooms were many times more heavily exposed than those sampled at working level, and the gradient was reversed. The greater exposure farther away from the light would seem to indicate circulation toward the wall at working level and in reversed direction above.

Several factors could account for differences between these two methods. Perhaps natural circulation between the chosen testing points was actually lower; but the small fan might also make a difference. Slight stratification by the mushrooming of air, cooled by evaporation of infected droplets, was shown in 24 runs by an increase of 30 per cent. in lethal exposure when a small heating element was suspended beneath the fan. Body warmth of occupants might similarly raise lethal exposure by increasing circulation.

Samples taken as a point two-thirds of the distance from the infector to the corner of the square room with the central hanging fixture compared more favorably with those taken by the previous method. The averages of 24 runs are shown in Chart V (lower). Exposure of the air in the upper level was hardly more than double that at the lower level—contrasting sharply with the large differences observed in the room with end wall fixtures. These observations would also seem to indicate more effective circulation through the irradiated core of the square room than through the more remote angles between the ceilings and the walls in the rectangular room.

AVERAGE LETHAL EXPOSURE.

A lethal gradient, L_a, theoretically represents a statistical average of exposures of organisms passing on an infinity of paths from infector to infectee. Our test actually gives a bacteriological average of the exposures of a large number of organisms carried on prevailing currents. The tests vary because of fluctuations in air circulation between fixed points. These fluctuations must also be averaged if a gradient is used as an index of sanitary ventilation.

Average lethal exposure, L, of organisms circulating from an occupied through an irradiated zone theoretically represents a statistical average of an infinity of gradients between occupants of a room. The average gradient derived in our studies was only 58 per cent. of the lethal gradient previously used as an index of sanitary ventilation.

Gradients from a number of infectors to a single sampling point can also be averaged bacteriologically. Average lethal exposure of test organisms atomized into four quadrants of a room is measured at the center. By compensating for directional circulation, the test averages disinfection gradients. The organisms are dispersed, with a minimum

of atmospheric stratification, or disturbance, from crowns of little orifices in small vaporizers.* In a series of nine comparative tests, the average lethal exposure given by the new method was 60 per cent. of lethal gradient formerly used as an index of sanitary ventilation, or about 3 per cent. higher than the average lethal gradient. This improved method simplifies the measurement of sanitary ventilation (Chart VI).

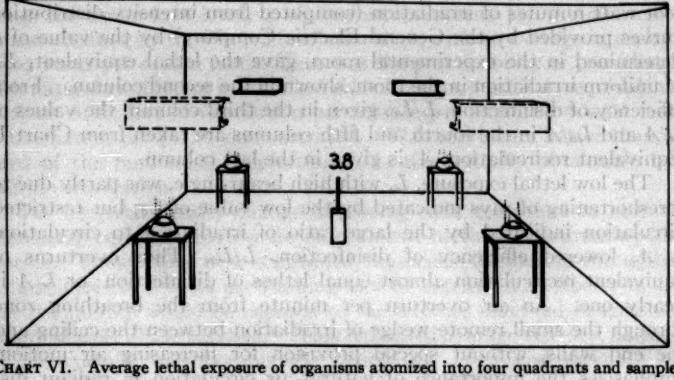

CHART VI. Average lethal exposure of organisms atomized into four quadrants and sampled at center of room. (Upper Chart IV, with low visored beam angle.)

EQUIVALENT RECIRCULATION.

Equivalent recirculation, A, for different light distribution in the rectangular room with end wall fixtures, has been derived in Table I.

TABLE I.

Equivalent Recirculation.

Beam Elevation	L	L_e	L/L_e	L_e/A	L/A	A
High.....	1.2	3.8	.31	3.1	.96	1.2
Low.....	8.2	12.8	.64	1.0	.62	12.8
Low with visor.....	3.7	10.2	.36	2.6	.96	3.9

L = negative natural logarithm of fraction of survivors.

L_e = 500 times product of mean ray length in feet, lethal flux in watts, and time in minutes, divided by room volume in cubic feet.

A = equivalent recirculation through irradiation, L_e, in air changes or overturns per minute.

The distribution of irradiation was varied, without altering circulation, by tilting the reflector upward or downward and by affixing a visor to the edge of the fixture. At high beam angle the corners between the

*As by the Fragrant-mist vaporizer manufactured by the Walton Laboratories, Inc., Irvington, N. J.

end walls and the ceiling were intensively irradiated, the air below the ceiling center less intensely from the flank of the beam. At low angle, a strong beam thrown across the room flooded the upper region above the seven-foot level, light from the flank of the beam spilling into the lower occupied zone. This flanking irradiation below the seven-foot level was then cut off by a visor, the flooded zone above remaining the same.

Average lethal exposure, L, is given in the first column. Multiplying foot watt minutes of irradiation (computed from intensity distribution curves provided by the General Electric Company) by the value of α determined in the experimental room, gave the lethal equivalent, L_0, of uniform irradiation in the room, shown in the second column. From efficiency of disinfection, L/L_0, given in the third column, the values of L/A and L_0/A in the fourth and fifth columns are taken from Chart I. Equivalent recirculation, A, is given in the last column.

The low lethal exposure, L, with high beam angle, was partly due to foreshortening of rays indicated by the low value of L_0; but restricted circulation indicated by the large ratio of irradiation to circulation, L_0/A, lowered efficiency of disinfection, L/L_0. Thus overturns of equivalent recirculation almost equal lethes of disinfection; or L/A is nearly one. An air overturn per minute from the breathing zone through the small remote wedge of irradiation between the ceiling and the end walls, without special provision for increasing air motion, emphasizes the importance of natural air circulation in radiant disinfection.

Lengthening rays with lower beam elevation increased irradiation more than three-fold; but the increase in disinfection of almost sevenfold emphasizes the importance of distributing irradiation. The tenfold increase in equivalent recirculation was due more to this distribution of irradiation than to actual circulation between irradiated and unirradiated zones. It contrasts the effect of passing light through air with circulation of air through light, in equivalent recirculation by radiant disinfection of air.

The erythemal tolerance of occupants did not permit direct irradiation of occupied zones, and approximately one-fifth of irradiation (below the seven-foot level) was cut off by a visor. This loss of direct irradiation of the occupied zone reduced equivalent recirculation more than three-fold, resulting in a net loss in lethal exposure of about a half. Yet even after sacrificing radiation, lowering beam elevation gained more than three-fold in lethal exposure.

CIRCULATION.

It makes little hygienic difference whether infection is destroyed by directing light through air or circulating air through light. But

utilization of natural circulation is all important in sanitary ventilation by indirect irradiation; for mechanical circulation is expensive and drafts must be avoided. The engineer must therefore differentiate between circulation and equivalent recirculation in realizing the full hygienic potentialities of radiant disinfection.

Effective circulation through the region most remote from the zone of occupancy (with high beam elevation) exceeded one overturn per minute in standard school rooms. Between the regions above and below the seven-foot level, 4 equivalent overturns per minute were almost attained by the visored low beam angle with an average intensity of .02 watts per square foot. Thus was the practicability of providing, with natural circulation in standard school rooms, a sanitary equivalent of 1,000 cubic feet of ventilation per minute per pupil, by 6 watt feet of irradiation per pupil, demonstrated. This represents better than a third of the maximum disinfection L/L_0 theoretically obtainable by uniform irradiation.

The bacterial density change in passing cubicle barriers on normal circulating currents provides an independent method of estimating air motion. If our value of α is assumed, organisms circulating through a radiant flux of .2 watts per running foot of barrier at a velocity of 16 feet per minute would be exposed to the 6 lethes observed in tests on experimental cubicle barriers.[9] This estimated average velocity, normal to the curtain, corroborates the ventilating engineers' estimate of optional air currents, approximately 30 feet per minute.

Circulation defined by these formulae should not, however, be construed too literally. The complete mixing assumed in the theory of dilution by air replacement cannot possibly be satisfied in the circulation of large masses of air between occupied and irradiated zones. Air turbulence theoretically steepens average disinfection gradients, yet large fans actually decreased four-fold the average lethal exposure as determined by the new method. Turbulence would however decrease exposure between infector and infectee if vertical circulation normally exceeds lateral mixing. Further analysis of sanitary ventilation by indirect irradiation will require a more detailed study of directional circulation.

SANITARY VENTILATION BY INDIRECT IRRADIATION.

Sanitary ventilation by indirect irradiation may now be compared with disinfection of recirculated air or ventilation with fresh air. With a high degree of disinfection L approaches A, and recirculated air becomes the sanitary equivalent of ventilation by an equal volume of fresh air. Likewise with high intensity of indirect irradiation L approaches A, as circulation approaches equivalent recirculation. Thus for $L/A = .96$, we may assume that three-fold increase in equivalent

recirculation at low visored beam angle represented actual circulation of three times as much air through the radiant beam; as by three-fold increase in the recirculation of disinfected air, or ventilation by fresh air.

The actual circulation of air was not affected by the change in beam angle, and the visor actually cut off some of the radiation. The effect of tripling recirculation of disinfected air, or ventilation with fresh air, was achieved by tripling the proportion of the air, circulating between the lower and upper regions, intercepted by rays of triple length. Thus were equivalent recirculation, irradiation, and average lethal exposure, all proportionately increased; one way that ray length, discussed in the preceding paper, increases radiant disinfection.

If, instead of increasing ray length, beam intensity had been increased three-fold, average lethal exposure would not change appreciably; for the same amount of air would circulate through the beam. If, on the other hand, ray length had been increased without changing the amount of irradiation (beam intensity being correspondingly reduced), lethal exposure would have been doubled, because of the greater volume of air circulating through the longer beam. Since efficiency of irradiation (defined in the preceding paper) is proportional to mean ray length, it bears the same relationship to efficiency of disinfection by indirect irradiation.

The significance of mean ray length in direct and indirect irradiation can now be compared. Both are but special cases of the general law of radiant disinfection—that the number of killed organisms is proportional to the radiant energy intercepted by living organisms. Maximum disinfection thus results from uniform exposure, either because of uniform distribution of light or living organisms. With non-uniform distribution of light, circulation makes for uniform exposure of surviving organisms; and with infinite circulation the maximum disinfection of uniform irradiation would be reached.

Equivalent recirculation then measures the approach to uniform lethal exposure, because of wider distribution of irradiation, or of more rapid mixing of the living organisms by air circulation—or the interdependence of both. With widening distribution of irradiation, therefore, the irradiated zone shrinks, until recirculation finally becomes the circulation of irradiated air through the unirradiated zone. Nor is the line of demarcation distinct, for equivalent recirculation in direct irradiation includes the circulation of less intensely irradiated air through more intense irradiation. Even though actual circulation is negligible, equivalent recirculation approaches infinity as uniformity of irradiation is approached. This is clearly illustrated by the high value of equivalent recirculation at low beam angle; and though the visor cut off only one-fifth of the irradiation (below the seven foot level), lethal exposure was reduced more than three-fold—another reason why ray length, or efficiency of irradiation, was emphasized in the preceding paper.

SANITARY SPECIFICATIONS.

Foot watts of irradiation can readily be computed [1] if the fixture designer gives the percentage of rated lethal flux radiated in each direction. Such computations would be facilitated if the irradiation engineer tabulated mean ray length for different distances of the fixture from the ceiling and walls. In the absence of such data, the sanitarian is usually justified in estimating L_0 by applying mean ray length in a vertical plane normal to the center of the tube.

As the art of irradiation develops, factors characterizing circulation of typical situations will accumulate; but until the ventilating engineer can fully define air circulation in occupied spaces, it will be necessary to integrate equivalent recirculation by the bacteriological procedure presented here. We have found four overturns per minute between the zones above and below the seven-foot level in the simple case of standard school rooms. Under similar conditions, the engineer is, therefore, justified in assuming A to be four times the efficiency of irradiation (mean ray length divided by the cube root of the volume) defined in the preceding paper.

The efficiency of disinfection, L/L_0, corresponding to L_0/A on Chart I, defines L, lethal exposure. If the architect, acting for the owner, specifies sanitary ventilation, the ventilating engineer reverses the calculation, translating the specifications into foot watts of irradiation required by the appropriate efficiency of irradiation, i.e., equivalent recirculation.

THRESHOLD SANITARY VENTILATION.

There but remains the hygienic specifications of sanitary ventilation—a bold project, indeed! Yet medical opinion has, within a decade, abandoned the conviction that air could be but an insignificant vehicle of infection—in favor of a theory that the indoor air we breathe in the winter accounts for most of our respiratory illness. Summer ventilation, on the contrary, will not support contagious epidemics. The maximum ventilation capable of maintaining infection introduced into aggregations of susceptible individuals is called *threshold sanitary ventilation*—the minimum hygienic specification.

Studies of the dynamic spread of measles in classrooms have indicated a threshold about five times normal winter ventilation [11] (i.e. about 5×30 cubic feet per pupil per minute by the Pennsylvania code), theoretically attainable by one foot watt per pupil with the efficiency of disinfection determined in this study. Considering how sensitive to moisture is the vulnerability of air-borne organisms exposed to lethal light, and practical exigencies of sanitary ventilation, and uncertain values assumed in the theory, good engineering dictates the fullest practicable utilization of available natural circulation. Six foot watts of irradiation per pupil have checked the dynamic spread

of measles in classrooms and, where the communication center of commerce in this contagion is the school, should control epidemics in the community. This hypothesis, that threshold communal sanitary ventilation will check epidemics of air-borne contagion in a community, is now being submitted to rigorous experiment.

SUMMARY.

1. An improved method of measuring sanitary ventilation has been developed. The average lethal exposure of air-borne infection between occupants of enclosed spaces measures air disinfection in terms of ventilation, a lethe of disinfection becoming the sanitary equivalent of an air change of ventilation.

2. Lethal exposure of *E. coli*, atomized into dry air, to 2537 Å radiation, has been revaluated. Exposure to .002 watt minutes per square foot, or .002 foot watt minutes per cubic foot of uniform irradiation, gives a lethe of disinfection, equivalent to an air change of ventilation. One foot watt minute of uniform irradiation becomes the sanitary equivalent of 500 cubic feet of fresh dry air.

3. The sanitary equivalent of irradiation of recirculated air has been formulated. Sanitary ventilation approaches recirculation as disinfection increases, and uniform irradiation of the room as recirculation increases. Recirculated air, to provide the approximate sanitary equivalent of fresh air, must be exposed to at least five times the direct irradiation in a room providing equivalent sanitary ventilation.

4. This formulation may also be applied to equivalent recirculation by indirect irradiation, combining air circulation through light with light passage through air.

5. By varying light distribution, the effective circulation between the occupied and the irradiated zone, below and above the seven-foot level in standard classrooms, was found to exceed four air changes a minute. The sanitary equivalent of 1,000 cubic feet of ventilation per minute per pupil was obtained by 6 foot watts of irradiation per pupil. This exceeds one-third of the maximum theoretical disinfection with uniformly distributed irradiation or infinite recirculation.

6. Specification of sanitary ventilation by radiant disinfection is simplified by this formulation.

ACKNOWLEDGMENT.

For technical assistance in the determination of lethal exposure by the original method and tests of cubicle barriers, I am indebted to Miss Ruth Blumfeld; by the second method, to Miss Dorothy Wells; for determination of lethal gradients, to Mr. Richard Greene and Miss Dorothy Wells; and for calibration of the new method, to Miss Cretyl Crumb and Mr. Peter Langer. The consistency of their results testifies

to the dependability of their work as well as to the practicability of the method.

For assistance in design of the experimental room and for its construction, I am indebted to Ensign Arthur E. Hammarlund, U.S.N.R.; and to Mrs. Elizabeth Rigney for technical assistance in making the tests.

REFERENCES.

1. WELLS, WILLIAM FIRTH. "Ray Length in Sanitary Ventilation by Bactericidal Irradiation of Air." *Jour. of Franklin Inst.*, **238**: 185–193, September, 1944.
2. WELLS, WILLIAM FIRTH. "Bactericidal Irradiation of Air. I. Physical Factors." *Jour. of Franklin Inst.*, **229**: 347–372, March, 1940.
3. WELLS, WILLIAM F. "Radiant Disinfection of Air." *Arch. Physiol. Therapy*, **23**: 143–148, March, 1942.
4. GATES, F. L. "A Study of the Bactericidal Action of Ultra-Violet Light. III. The Absorption of Ultra-Violet Light by Bacteria." *J. Gen. Physiol.*, **14**: 31, 1930. HOLLAENDER, A. AND CLAUS, W. D. "The Bactericidal Effect of Ultra-Violet Radiation of *Escherichia coli* in Liquid Suspensions." *J. Gen. Physiol.*, **19**: 753, 1936. DREYER, G. AND CAMPBELL-RENTON, M. L. "A Quantitative Study of the Action of Ultra-Violet Light on Bacteria." *Proc. Royal Soc. London*, Ser. B, **120**: 447, 1936. COBLENTZ, W. W. AND FULTON, H. R. "A Radiometric Investigation of the Germicidal Action of Ultra-Violet Radiation." Scientific Papers of the Bureau of Standards, No. 495.
5. WELLS, W. F. AND FAIR, G. M. "Viability of *B. coli* Exposed to Ultra-Violet Radiation of Air." *Science*, **82**: 280, 1935. WELLS, W. F. "Air-borne Infection and Sanitary Air Control." *J. Indust. Hyg. and Toxicol.*, **17**: 253–257, November, 1935.
6. WHISLER, B. A. "The Efficacy of Ultra-Violet Light Sources in Killing Bacteria Suspended in Air." *Iowa State College J. Science*, **14**: 215–231, April, 1940.
7. FORSYTHE, W. F., BARNES, B. T., AND EASLEY, M. A. "Ultra-Violet Sources and Their Radiation." *J. Optical Soc. Amer.*, **24**: 178, 1934. BARNES, B. T. AND FORSYTHE W. F. "Characteristics of Some New Mercury Arc Lamps." *J. Optical Soc. Amer.*, **27**: 84, 1937. BUTTOLPH, L. J. *R.S.I.*, **1**: 487, 1930.
8. WELLS, W. F. AND WELLS, M. W. "The Measurement of Sanitary Ventilation." *Amer. J. Pub. Health*, **28**: 343–350, March, 1938.
9. WELLS, W. F. AND GREEN, R. "Bacteriologic Study of Radiant Disinfection of Air in the Control of Epidemic Spread of Contagion." Paper read before A. P. H. A., Oct. 14, 1941.
10. WELLS, W. F. "Air-borne Infection and the Use of Ultra-Violet Barriers." Colloquium, University of Notre Dame, 1939. Micrurgical and Germ-Free Methods by J. A. Reyniers, Charles C. Thomas, Publisher, 1943.
11. WELLS, W. F. AND WELLS, M. W. "Dynamics of Air-Borne Infection." *A. J. Med. Sc.*, **206**: 11–17, July, 1943.

Distilling Efficiency Improved.—An improvement in distilling efficiency contributing to accelerated production of ethyl alcohol for synthetic rubber manufacture and beverage spirits has been achieved at General Distillers Corporation of Kentucky, Louisville, by the use of Fiberglas tower packing in a fusel oil decanter.

To meet government standards requiring removal of fusel oil, distillers have long used a conventional type of tower construction equipped with metal baffles. W. H. Stone, production superintendent of General Distillers, reports that by equipping a decanter with random-oriented glass fiber packs, his firm has been able to save construction materials by using supports of lighter gauge, to step up production of fusel oil "very satisfactorily," and to eliminate the labor previously needed for subsequent purification of the oil.

Mr. Stone describes the decanter's design as a radical innovation in the distilling industry. The decanter, which handles the distillate from approximately 2,000 bushels of grain daily, is 15 feet high, 22 inches in diameter. It has more than ample capacity, and eliminates the need for large storage tanks required for aftertreatment of the fusel oil. Fusel oil as high as 98 per cent. pure has been produced by the decanter.

The negligible weight of the Fiberglas packing, Mr. Stone says, means that in designing supports for the column, only the weight of the liquid to be handled needs to be considered.

Mr. Stone attributes the superior performance of the newly installed decanter to the large surface area afforded by the glass fiber packs. The packs are similar to those used for filtration, evaporation, absorption and fractionation purposes by many process industries. Supplied by Owens-Corning Fiberglas Corporation, the packs have an average surface area of approximately 196 square feet per cubic foot.

The decanter at General Distillers is packed with 80 cubic feet of the Fiberglas tower packing which is installed at a density of 5 pounds per cubic foot. Thus, as the liquids (water, fusel oil and alcohol) rise in the decanter, they encounter approximately 15,680 square feet of area—approximately three-eighths of an acre—which effectively intermixes the ingredients and washes the fusel oil free of alcohol.

The surface area, afforded by 400 pounds of glass fiber packs, is many thousands of times the area provided in a decanter of conventional design.

R. H. O.

THE ELECTRICAL CONSTANTS OF THE ELECTRO-MAGNETIC MICROBAROGRAPH.

BY

EUGENE L. SULKOWSKI.

The work presented by this paper was completed at the Seismological Laboratory of the University of Pittsburgh previous to the author's enlistment as a Meteorological Cadet in the United States Army Air Forces.

This paper is a supplement to "The Calibration of the Electromagnetic Microbarograph," and presents a method used to control the sensitivity of this instrument.[1] The microbarograph, during the course of calibration, was operated at full sensitivity. Before it can be used to record data, a sensitivity control must be devised.

At the time of initial calibration, the circuit consisted of the microbarograph coil, a resistance (R_0), and the galvanometer (Fig. 1). By

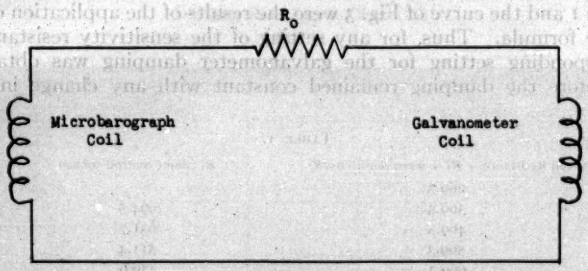

FIG. 1.

means of the coil and R_0, the galvanometer was critically damped. To control the sensitivity, a Leeds and Northrup resistance box was inserted at A (Fig. 2). It is apparent that if the sensitivity resistance were changed, the damping ratio would also change. To obtain critical damping at any given change in sensitivity, another Leeds and Northrup resistance box was inserted at B (Fig. 2).

Since the sensitivity resistance was in series with the constant resistances of the coil and R_0 (now combined with the sensitivity resistance) and the damping control shunts the galvanometer, the net-

[1] Sulkowski, Eugene L., "The Calibration of the Electromagnetic Microbarograph," JOURNAL OF THE FRANKLIN INSTITUTE, Vol. 235, No. 3 (March, 1943).

work became a parallel circuit to which Ohm's law was applied.

$$1/R_3 = 1/R_2 + 1/R_1 \qquad \text{or} \qquad R_1 = \frac{R_2 R_3}{R_2 - R_3}.$$

Letting R_1 = shunt resistance to obtain critical damping,
R_2 = (coil resistance) + (given sensitivity resistance),
R_3 = 269.3 ohms (constant resistance for critical damping).

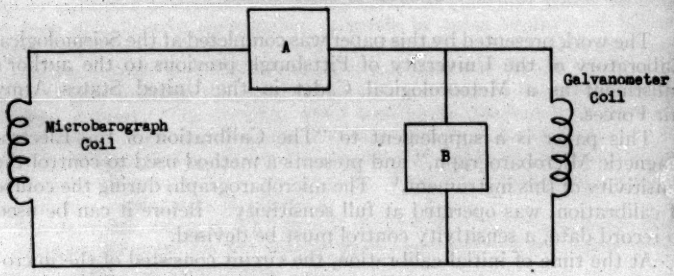

FIG. 2.

Table 1 and the curve of Fig. 3 were the results of the application of the above formula. Thus, for any setting of the sensitivity resistance, a corresponding setting for the galvanometer damping was obtained. Therefore the damping remained constant with any change in sensitivity.

TABLE 1.

R_3 (coil Resistance + R_2 + given sensitivity R)	R_1 (shunt control) (ohms)
269.3	—
369.3	994.5
469.3	631.7
569.3	511.4
669.3	450.6
769.3	414.3
869.3	390.1
969.3	372.9
1069.3	359.8
1169.3	349.8
1269.3	341.8
1369.3	335.2
1469.3	329.7
1569.3	325.0
1669.3	320.8

To find the change in trace amplitude corresponding to a change in sensitivity resistance, a series of records was obtained by the following method: The microbarograph and calibration equipment were prepared as for calibration, with the exception that the micromanometer was not

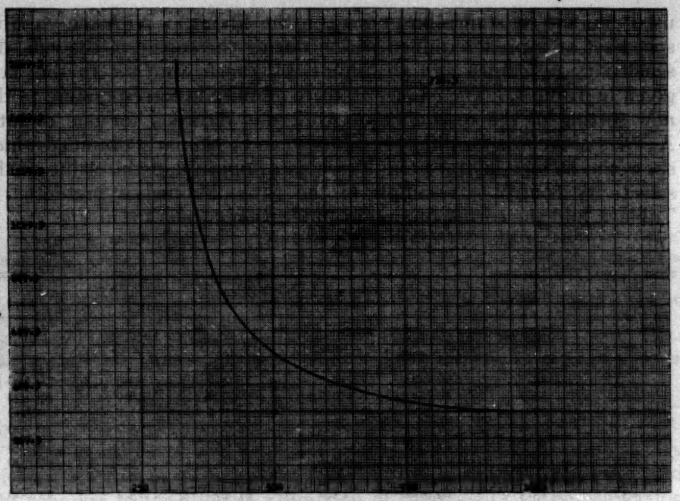

Damping Resistance in Ohms (R_1)

FIG. 3.

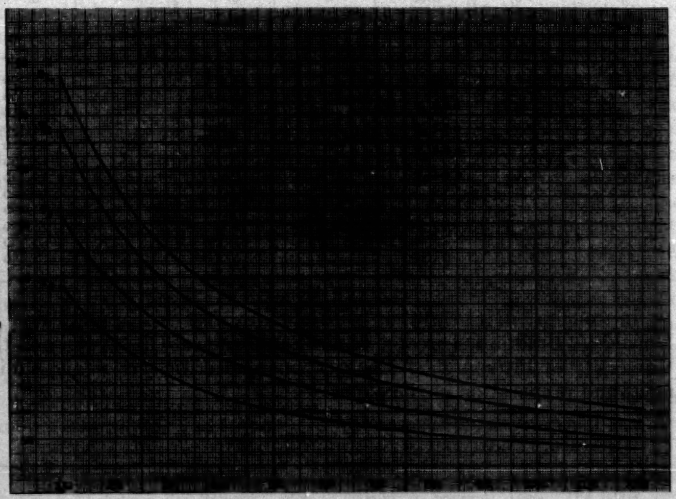

Sensitivity Resistance in Ohms (Box A)

FIG. 4.

used and the resistance boxes were in the circuit.[2] With the variable speed set at a predetermined period during the course of the run, the sensitivity resistance and the shunt resistance were set to the data given in Table 1. The change in trace amplitude corresponding to the new setting of the resistance network was recorded for one minute. A series of records for different periods can be similarly obtained which show the change in trace amplitude as a function of the value of the sensitivity control. A sample of the data obtained is presented in Table 2, and the corresponding magnification curves are in Fig. 4.

TABLE 2.

Ohms (R_A)	Period = 2 seconds		Period = 2.75 seconds		Period = 4 seconds	
	Amplitude (mm.)	Magnification	Amplitude (mm.)	Magnification	Amplitude (mm.)	Magnification
132	46.7	66,600	52.5	75,000	53.5	76,500
232	34.7	49,600	39.5	56,500	40.0	57,100
332	27.4	39,200	30.9	44,100	31.0	44,300
432	22.6	32,240	25.6	36,600	25.7	36,700
532	19.7	28,170	21.6	30,840	22.0	32,700
632	16.9	24,400	18.8	26,840	19.2	27,400
732	14.9	21,300	16.7	23,840	17.0	24,300
832	13.3	19,000	15.0	21,400	15.2	21,800
932	12.0	17,150	13.6	19,400	13.9	19,950
1032	11.0	15,710	12.6	18,000	12.7	18,300
1132	10.2	14,570	11.5	16,450	11.5	16,400
1232	9.5	13,530	10.6	15,150	10.7	15,600
	Period = 5.7 seconds		Period = 8 seconds		Period = 11.6 seconds	
132	46.25	66,100	36.0	51,490	26.6	38,000
232	34.25	48,900	26.75	38,200	19.3	27,560
332	27.0	38,600	21.0	30,000	15.2	21,750
432	22.5	31,700	17.5	25,000	13.0	18,560
532	19.0	27,190	14.75	21,060	11.1	15,500
632	16.5	23,800	13.0	18,570	9.7	13,760
732	14.5	20,650	11.5	16,420	8.7	12,420
832	13.0	18,580	10.25	14,640	7.6	10,860
932	11.75	16,800	9.5	13,550	7.0	10,000
1032	10.75	15,350	8.5	12,140	6.2	8,850
1132	10.0	14,300	7.75	11,080	5.8	8,290
1232	9.25	13,210	7.0	10,000	5.7	8,150

In conclusion, the author wishes to express his appreciation to Donald C. Bradford, Director of the Seismological Observatory of the University of Pittsburgh, for suggestions and criticisms on the equipment and preparation of the paper.

THE UNIVERSITY OF PITTSBURGH,
PITTSBURGH, PENNSYLVANIA.

[2] E. L. Sulkowski, op. cit., p. 253.

SIMPLIFIED EQUATIONS OF INTERIOR BALLISTICS.

BY

JOSEPH E. MAYER * AND B. I. HART,

Ballistic Research Laboratory, Aberdeen Proving Ground.

ABSTRACT.

Subject to the assumptions of zero starting pressure, covolume equal to charge volume, burning rate proportional to pressure, constant burning surface, and no heat loss through gas or projectile friction, the equations of interior ballistics are presented in simple form.

It is hoped that these simple equations will be of some aid in making ready approximate evaluations of the effect of variation of any parameter.

The general equations are listed in section I. In section II the expressions for the maximum pressure and muzzle velocity are discussed more fully, and the derivatives with respect to various parameters are given.

I. THE GENERAL EQUATIONS.

The equations of interior ballistics are used to calculate the velocity of the projectile as a function of travel in the bore of the gun tube, and the pressure in the tube as a function of the travel.† The conversion to pressure as a function of time is important for some problems, such as recoil, and is always possible if the two functions mentioned above are available. In this paper equations are given for the velocity-travel and pressure-travel curves, but not for the pressure-time relationship.

The projectile is propelled by the pressure of gas acting on its base. The pressure of gas is affected by the amount of charge burnt, which in turn is a function of the past pressure-time relation, since the rate of burning of propellants depends on the pressure. The equation of state of the gas, $p(v - cb) = cRT$, is commonly used (with p = pressure, v = volume, b = a temperature-independent covolume of the gas, c = charge, R = a constant, and T = absolute temperature). The temperature of the gas is T_0 if no work has been done and no heat lost. This temperature is referred to as the adiabatic flame temperature. The somewhat inconsistent term specific force, or just force, λ, is used for the product RT_0. The specific heat of the gas is implicitly included by giving the ratio of specific heats γ, so that the decrease in pv due to the loss of energy of the gas is equal to $(\gamma - 1)$ times the energy loss (equation (5)).

The propellent charge of a gun is in the form of powder grains of known size and shape. Each of these grains burns on its surface,

* Also Department of Chemistry, Columbia University.

† T. J. Hayes, "Elements of Ordnance," New York, John Wiley & Sons, Inc., 1938. C. Cranz, "Lehrbuch der Ballistik," Vol. II, Berlin, J. Springer, 1926. The latter work contains an extensive bibliography.

which recedes parallel to itself at a rate dependent on the gas pressure. Thus the actual development of gas depends on the geometry of the grains, and grains are used for which the surface decreases (regressive grains) during burning, stays constant (constant burning grains) or even increases (progressive grains). The treatment here is for grains of constant burning surface. The grains are usually described by giving their "web," w, which is essentially their thickness, that is, twice the amount of surface regression necessary before two opposite burning surfaces come into contact.

The loss of efficiency through heat conduction and friction is not large in artillery weapons, and is neglected here. In actual rifled weapons the projectile starts to move only after the pressure exceeds a certain "starting pressure," an effect which is also neglected in what follows.

The differential equations, which are set up in accord with the commonly used physical hypotheses, are usually solved by numerical integration, and the results tabulated for various values of the many parameters involved. By a suitable choice of assumptions relatively simple analytical solutions may be obtained. These are convenient, even if highly approximate.

We use the symbols

a = cross section of the bore (ins.)^2.
b, as a subscript, indicates all burnt.
c = charge burnt (lbs.).
C = total charge (lbs.).
g = gravitational constant = 386.4 in./sec.^{2}
m, as a subscript, refers to muzzle.
max, as a subscript, refers to maximum pressure.
p = pressure (lbs./in.^{2}).
p_e = a constant of the dimensions of pressure (lbs./in.^{2}).
p_q = a constant of the dimensions of pressure (lbs./in.^{2}).
q = burning constant (surface recession (ins./sec.) = $q \times$ pressure (lbs./in.^{2})).
T = temperature, absolute, of the powder gases.
T_0 = the adiabatic flame temperature.
u = velocity of the projectile (ft./sec.).
v = volume behind projectile base minus charge volume (ins.)^3.
v_e = chamber volume (ins.)^3.
v_0 = chamber volume minus original charge volume (ins.)^3.
W = projectile weight plus one third C (lbs.).
w = web (ins.).
γ = ratio of specific heats.
λ = specific force of propellant (ins.); this is defined as the pressure volume product of unit weight of propellant if burned without loss of energy.

We assume:

(1) that the starting pressure is zero; that is, that the projectile starts to move immediately the powder begins to burn and that the pressure necessary to engrave the band is zero,

(2) that the covolume of the propellent gases is equal to the original charge volume,

(3) that the chemical burning rate of the propellant is proportional to the first power of the pressure,

(4) that the area of the surface of the propellant remains constant during the burning,

(5) that no heat or energy is lost through conduction or through friction.*

The burning of a propellant is given by the statement that the rate of recession $\dot{z}$ of the burning surface of the grain is a function of the pressure, and we choose

$$\dot{z} = qp, \tag{1}$$

with q the burning constant of the powder. The amount, $\dot{c}$, of charge burnt per unit time is $\dot{z}\rho\sigma$, where ρ is the propellant density and σ its surface. Since the propellant is assumed to be of such a shape that its surface remains constant (for instance, sheets of area $\gg$ than thickness squared) the volume of the propellant is initially $(w\sigma/2)$ with w the web or thickness, and the initial charge C is $(\rho w\sigma/2)$. One then has $\rho\sigma = 2C/w$ and

$$\dot{c} = C(2\dot{z}/w) = C(2qp/w) \tag{2}$$

from (1).

The specific force λ of the propellant is the product of p and the free volume for the uncooled gases produced from unit weight of propellant. The free volume of the chamber, v_0, is

$$v_0 = v_c - 17.7C \tag{3}$$

where 17.7 is the average volume in cubic inches of one pound of propellant, and the free volume behind the projectile base, v, is

$$v = v_0 + 12as \tag{4}$$

where s is the travel in feet.

* The common procedure for taking care of the energy losses due to friction and heat is by changing the value of γ, as suggested by R. H. Kent. If this is done Dr. J. P. Vinti and Mr. J. Chernick have found that the agreement between this simple theory and more elaborate theories, as judged by the ratio of muzzle energy to maximum pressure, is of the order of one per cent. The maximum pressure, however, may be somewhat more in error, the amount of error depending on the manner of transforming the burning rate coefficient appropriate to a more accurate burning law to a value for use in the first power burning law. If the burning law should be $q_2p^{0.8}$ instead of qp and the correspondence is made by equating qp to $q_2p^{0.8}$ at maximum pressure, the discrepancy in maximum pressure may amount to as much as 30 per cent. On the other hand, if the correspondence is made at $\frac{1}{2}p_{max}$, the discrepancy may be only a few per cent.

The pressure is related to the free volume v, the amount of powder burnt c, and the velocity of the projectile u by

$$pv = c\lambda - (\gamma - 1)(W/2g)(12u)^2 \tag{5}$$

where $(W/2g)(12u)^2$ is the energy of the projectile, which has all come at the expense of the energy of the propellent gases. Since W includes one-third of the charge weight C, as well as the projectile weight, there is included as "projectile energy" the kinetic energy of motion of the propellent gases. The factor one-third arises from the fact that, if their density distribution down the tube is uniform, the average of the square of the velocity of the gases is one-third the velocity of the projectile squared.

The equation of motion of the projectile is

$$(W/g)(12\dot{u}) = pa. \tag{6}$$

The three equations, (2), (5), and (6) are our fundamental equations. We define

$$p_q = (2qC\lambda/aw)^2(W/gv_0), \tag{7}$$

$$p_c = C\lambda/v_0, \tag{8}$$

both of the dimensions of pressure, the latter being the pressure which would be developed in the chamber if the complete charge burnt before motion of the projectile, that is, with instantaneous combustion.

From (2), since the initial charge burnt is zero, we see that c is proportional to $\int p dt$, whereas from (6) it is seen that u is also proportional to the same integral. The velocity of the projectile is therefore always proportional to the charge burnt up to complete combustion. Using (7) and (8) the relationship can be expressed as

$$c\lambda = \left(\frac{c}{C}\right) p_c v_0 = \sqrt{p_q v_0 (W/g)}(12u) \tag{9}$$

or

$$(W/2g)(12u)^2 = \frac{1}{2}\left(\frac{c}{C}\right)^2 p_c v_0 \left(\frac{p_c}{p_q}\right). \tag{9'}$$

Equation (5) may then be written

$$p(v/v_0) = p_c(c/C)\left[1 - \frac{\gamma - 1}{2}\left(\frac{p_c}{p_q}\right)\left(\frac{c}{C}\right)\right]. \tag{10}$$

We use $du/dt = (du/ds)(ds/dt) = u(du/ds) = 12au du/d(12as) = 12au(du/dv)$, or from (6)

$$p = (W/ga)(12\dot{u}) = (W/g)(12u)d(12u)/dv, \tag{11}$$

and from (9),

$$p = p_c v_0 (p_c/p_q)(c/C)(d/dv)(c/C). \tag{12}$$

With this (10) becomes

$$\frac{d(c/C)}{d\ln v} = \frac{p_q}{p_e} - \frac{\gamma - 1}{2}\frac{c}{C}, \tag{13}$$

$$\ln(v/v_0) = \int_0^{c/C} \frac{dx}{(p_q/p_e) - \frac{1}{2}(\gamma - 1)x} = -\frac{2}{\gamma - 1}\ln\left[1 - \frac{\gamma - 1}{2}\frac{p_e}{p_q}\frac{c}{C}\right]. \tag{13'}$$

Then the relation between c/C, the fraction of the charge burnt, and v/v_0, the expansion ratio, is

$$v/v_0 = [1 - \tfrac{1}{2}(\gamma - 1)(p_e/p_q)(c/C)]^{-2/(\gamma-1)} \tag{14}$$

$$c/C = [2p_q/p_e(\gamma - 1)][1 - (v/v_0)^{-(\gamma-1)/2}]. \tag{14'}$$

The pressure-expansion ratio equation is, from (10) and (14'):

$$p = [2/(\gamma - 1)]p_q(v/v_0)^{-\gamma}[(v/v_0)^{\frac{1}{2}(\gamma-1)} - 1]. \tag{15}$$

The pressure is a maximum when:

$$v_{max}/v_0 = [2\gamma/(\gamma + 1)]^{2/(\gamma-1)}, \tag{16}$$

$$c_{max}/C = p_q/\gamma p_e, \tag{16'}$$

and has the value:

$$p_{max} = p_q[(\gamma + 1)^{(\gamma+1)}\gamma^{-2}2^{-(\gamma+1)}]^{1/(\gamma-1)}. \tag{17}$$

The function $f(\gamma) = [(\gamma + 1)^{(\gamma+1)}\gamma^{-2}2^{-(\gamma+1)}]^{1/(\gamma-1)}$ is $1/e$ for $\gamma = 1$. It does not vary greatly with γ having values:

γ	$f(\gamma)$	γ	$f(\gamma)$
1.0	0.368	1.25	0.310
1.05	0.355	1.30	0.301
1.10	0.342	1.35	0.292
1.15	0.331	1.40	0.283
1.20	0.320		

It is closely approximated by $f(\gamma) \cong e^{-1}[1 + \frac{3}{4}(\gamma - 1)]^{-1}$, the agreement being to at least three significant figures for values of γ to 1.40.

The values of v_{max}/v_0 for different values of γ are:

γ	v_{max}/v_0	γ	v_{max}/v_0
1.0	2.72	1.25	2.32
1.05	2.62	1.30	2.26
1.10	2.54	1.35	2.21
1.15	2.46	1.40	2.16
1.20	2.39		

In terms of the expansion ratio, before all the propellant is consumed, the energy of the projectile, from (9′) and (14′), is:

$$\frac{W}{2g}(12u)^2 = \frac{1}{5.37}Wu^2 = [2p_q v_0/(\gamma-1)^2][1-(v/v_0)^{-(\gamma-1)/2}]^2 \quad (18)$$

and the velocity is

$$u = \sqrt{10.74 p_q v_0/W}\,\frac{1}{\gamma-1}[1-(v/v_0)^{-(\gamma-1)/2}]. \quad (19)$$

The position of all burnt is given by $c/C = 1$, which from (14) is

$$v_b = v_0[1-\tfrac{1}{2}(\gamma-1)(p_c/p_q)]^{-2/(\gamma-1)}, \quad (20)$$

and this may be approximated by:

$$v_b = v_0 e^{p_c/p_q}\left\{1+\frac{1}{4}(\gamma-1)(p_c/p_q)^2 + \frac{1}{8}(\gamma-1)^2\left[\frac{2}{3}(p_c/p_q)^3+\frac{\gamma}{4}(p_c/p_q)^4\right]+\cdots\right\}. \quad (20^*)$$

The pressure at all burnt is:

$$p_b = p_c[1-\tfrac{1}{2}(\gamma-1)(p_c/p_q)]^{(\gamma+1)/(\gamma-1)} \quad (21)$$

which may be approximated by:

$$p_b = p_c e^{-(p_c/p_q)}[1-\tfrac{1}{2}(\gamma-1)(p_c/p_q)-\tfrac{1}{4}(\gamma-1)(p_c/p_q)^2+\cdots]. \quad (21^*)$$

The energy of the projectile at burnt is:

$$\frac{1}{5.37}Wu_b^2 = \frac{1}{2}C\lambda(p_c/p_q), \quad (22)$$

and the velocity is

$$u_b = \sqrt{2.68(C\lambda/W)(p_c/p_q)}. \quad (22')$$

Beyond the position of burnt the gases obey the equation of adiabatic expansion, pv^γ is constant, so that at the muzzle the pressure is $(v_b/v_m)^\gamma p_b$, and from (21),

$$p_{\text{muzzle}} = p_c(v_0/v_m)^\gamma[1-\tfrac{1}{2}(\gamma-1)(p_c/p_q)]^{-1}. \quad (23)$$

The muzzle energy is given by:

$$\frac{1}{5.37}Wu_m^2 = \frac{C\lambda}{\gamma-1}\left\{1-(v_0/v_m)^{\gamma-1}\left[1-\frac{1}{2}(\gamma-1)(p_c/p_q)\right]^{-1}\right\}, \quad (24)$$

* Equations marked by asterisk are approximate expansions which are valid for most weapons.

which may be approximated as:

$$\frac{1}{5.37} W u_m^2 = C\lambda \left\{ \left[\ln (v_m/v_0) - \frac{1}{2} (p_c/p_q) \right] - \frac{1}{2} (\gamma - 1) \left[\ln^2 (v_m/v_0) - (p_c/p_q) \ln (v_m/v_0) + \frac{1}{2} (p_c/p_q)^2 \right] + \cdots \right\}. \quad (24^*)$$

The temperature (absolute) at the muzzle is

$$T_m = T_0 (v_0/v_m)^{\gamma-1} [1 - \tfrac{1}{2}(\gamma - 1)(p_c/p_q)]^{-1} \quad (25)$$

where T_0 is the adiabatic flame temperature of the propellant, that is, the temperature of the uncooled gases produced in the combustion.

II. THE MUZZLE VELOCITY AND MAXIMUM PRESSURE.

Of the equations listed those giving the maximum pressure, (17), and the muzzle energy, (24), are of the greatest practical importance.

The maximum pressure is given by (17) which may be approximated, to far greater accuracy than the theory warrants, by the simple form

$$p_{max} = (p_q/e)[1 + \tfrac{3}{4}(\gamma - 1)]^{-1} \quad (26)$$

where $e = 2.718$ is the base of the natural logarithm system. Since

$$p_q = (2qC\lambda/aw)^2 [W/g(v_c - 17.7C)], \quad (27)$$

it is seen that the maximum pressure is proportional to the projectile weight, depends on the charge as $C^2 \Big/ \left(1 - \frac{17.7C}{v_c}\right)$, depends on burning rate as q^2, on web as w^{-2}, and on the specific force of the propellant as λ^2. The dependence on the chamber volume is as $1/(v_c - 17.7C)$.

Since the burning rate q may be regarded as the least well known of the parameters entering this simplified form of the theory one may use the maximum pressure to determine q, or, more simply, to determine the parameter p_q:

$$p_q = 2.718 p_{max} [1 + \tfrac{3}{4}(\gamma - 1)]. \quad (28)$$

The equation for the muzzle energy, in inch lbs., may be made to appear simpler by defining the new symbols:

$$\tau = \ln (v_m/v_0) = 2.303 [\log_{10} (12as + v_c - 17.7C) - \log_{10} (v_c - 17.7C)], \quad (29)$$

$$\varphi = p_c/2p_q = (4.02/W)(aw/q)^2 (1/C\lambda), \quad (30)$$

$$h = \tau - \varphi, \quad (31)$$

$$E_m = \frac{1}{5.37} W u_m^2, \quad (32)$$

which latter is the muzzle energy in inch lbs., if the projectile weight, W, is in lbs., and the muzzle velocity, u_m, in feet per second.

In view of (28) φ may be determined from the maximum pressure as

$$\varphi = p_c/\{2ep_{max}[1 + \tfrac{3}{4}(\gamma - 1)]\}$$
$$= C\lambda/\{[v_c - 17.7C]5.436p_{max}[1 + \tfrac{3}{4}(\gamma - 1)]\}. \quad (33)$$

This equation is valid only if the point of all burnt comes later than the maximum pressure, which requires that

$$\varphi \leqq 1/2\gamma \qquad [\leqq 0.4 \quad \text{if} \quad (\gamma = 1.25)]. \quad (33')$$

The gun will "spit powder" unless the position of all burnt is before the muzzle. This requires that

$$-\ln[1 - (\gamma - 1)\varphi] \leqq \frac{\gamma - 1}{2} r, \quad (33'')$$

or approximately,

$$\varphi \leqq \tfrac{1}{2}r.$$

The quantity $h = r - \varphi$ is seen to be positive, and equal to or greater than φ, if the gun does not "spit powder."

The equation (24) for the muzzle energy becomes

$$E_m = \frac{C\lambda}{\gamma - 1}\{1 - e^{-(\gamma-1)r}[1 - (\gamma - 1)\varphi]^{-1}\} \quad (34)$$

which may be expanded to the forms

$$E_m = C\lambda\Big[(r - \varphi) - \frac{1}{2}(\gamma - 1)(r^2 - 2r\varphi + 2\varphi^2)$$
$$+ \frac{1}{6}(\gamma - 1)^2(r^3 - 3r^2\varphi + 6r\varphi^2 - 6\varphi^3)$$
$$- \frac{1}{24}(\gamma - 1)^3(r^4 - 4r^3\varphi + 12r^2\varphi^2 - 24r\varphi^3 + 24\varphi^4)\cdots\Big] \quad (34^*)$$

$$E_m = C\lambda\Big[h - \frac{1}{2}(\gamma - 1)(h^2 + \varphi^2)$$
$$+ \frac{1}{6}(\gamma - 1)^2(h^3 + 3h\varphi^2 - 2\varphi^3)$$
$$- \frac{1}{24}(\gamma - 1)^3(h^4 + 6h^2\varphi^2 - 8h\varphi^3 + 9\varphi^4)\cdots\Big]. \quad (34^{**})$$

Except for very long guns the first two terms

$$E_m = C\lambda h\{1 - \tfrac{1}{2}(\gamma - 1)[h + (\varphi^2/h)] + \cdots\} \quad (34^{***})$$

are sufficient, within an accuracy to which this simple theory applies.

From (34**) it is seen that for guns of moderate length (v_m/v_0 about 20, r about 3 and h about 2), the muzzle energy is proportional to the total "force" of the powder, the product of charge C and the specific force λ, and relatively independent of the value of γ. Since the potential of the powder is $\lambda/(\gamma - 1)$, this quantity for fixed force is highly dependent on γ. That is, the specific force λ, rather than the potential $\lambda/(\gamma - 1)$, represents the capacity of the propellant to do work in the gun, and is a more useful characteristic of the propellant on which to base comparisons of different compositions than the potential.

The variation of muzzle energy E_m, and muzzle velocity u_m, with the various parameters may be most conveniently expressed as logarithmic derivatives, which give the per cent. change in E_m or u_m with unit per cent. change in the parameter. Regarding charge C, projectile weight W, web w, burning constant q, specific heat ratio γ, and specific force λ as parameters, for a given gun (fixed v_c, a, and s) the logarithmic derivatives are as follows:

We use

$$j = \frac{C\lambda}{E_m}\left[1 - (\gamma - 1)\frac{E_m}{C\lambda}\right] = \frac{C\lambda}{E_m} - (\gamma - 1)$$

$$= \frac{1}{h}\left\{1 + \frac{1}{2}(\gamma - 1)[h + (\varphi^3/h) - 2] + \frac{1}{12}(\gamma - 1)^2[h^2 + 4\varphi^3/h + 3\varphi^4/h^2] + \cdots\right\}. \quad (35)$$

This parameter has a value in the neighborhood of 1/2, for most guns.

The per cent. change in muzzle energy for unit per cent. change in projectile weight is, using the conventional designation in thermodynamics of indicating by subscripts to the partial derivatives that web and burning rate are held constant,

$$(\partial \ln E_m/\partial \ln W)_{w,q} = j\varphi[1 - (\gamma - 1)\varphi]^{-1}, \quad (36)$$

and the per cent. change in muzzle velocity is

$$(\partial \ln u_m/\partial \ln W)_{w,q} = \tfrac{1}{2}\{j\varphi[1 - (\gamma - 1)\varphi]^{-1} - 1\}. \quad (36')$$

For all other parameters the per cent. change in muzzle velocity is just half the per cent. change in muzzle energy. The effect of change is

$$\left(\frac{\partial \ln E_m}{\partial \ln C}\right)_{w,q} = 2\frac{\partial \ln u_m}{\partial \ln C}$$

$$= 1 + j\left\{\frac{\varphi}{1 - (\gamma - 1)\varphi} + \frac{17.7C}{v_c}\left[1 + \frac{v_c - 17.7C}{12as_m}\right]^{-1}\left[1 - \frac{17.7C}{v_c}\right]^{-1}\right\}. \quad (37)$$

The changes due to web, w, and burning rate, q, are equal in magnitude and opposite in sign:

$$\frac{\partial \ln E_m}{\partial \ln q} = -\frac{\partial \ln E_m}{\partial \ln w} = 2\frac{\partial \ln u_m}{\partial \ln q} = -2\frac{\partial \ln u_m}{\partial \ln w} \tag{38}$$
$$= 2j\varphi[1-(\gamma-1)\varphi]^{-1}.$$

The changes due to force are:

$$\left(\frac{\partial \ln E_m}{\partial \ln \lambda}\right)_{w,q} = 2\frac{\partial \ln u_m}{\partial \ln \lambda} = 1 + j\varphi[1-(\gamma-1)\varphi]^{-1}. \tag{39}$$

If the powder characteristics, projectile weight, and other dimensions of the gun are held constant we have

$$\left(\frac{\partial \ln E_m}{\partial \ln v_c}\right)_{w,q} = 2\frac{\partial \ln u_m}{\partial \ln v_c}$$
$$= -j\left[1+\frac{v_c-17.7C}{12as_m}\right]^{-1}\left[1-\frac{17.7C}{v_c}\right]^{-1} \tag{40}$$

for the effect of the chamber capacity, v_c, and

$$\left(\frac{\partial \ln E_m}{\partial \ln s_m}\right)_{w,q} = 2\frac{\partial \ln u_m}{\partial \ln s_m} = j\left[1+\frac{v_c-17.7C}{12as_m}\right]^{-1} \tag{41}$$

for the effect of the travel, s_m, from the seating of the projectile to the muzzle.

If, instead of considering the parameters as C, W, w, q, λ and those of the gun, we take C, W, λ, p_{max} and those of the gun, it is equivalent to assuming that the web, or burning rate, or both, are varied to fix the maximum pressure. In this case we shall indicate the logarithmic derivatives by partials with the subscript p, to indicate that the maximum pressure is held constant. The results are:

$$(\partial \ln E_m/\partial \ln W)_p = 0, \tag{42}$$

$$(\partial \ln u_m/\partial \ln W)_p = -\frac{1}{2}, \tag{42'}$$

$$\left(\frac{\partial \ln E_m}{\partial \ln C}\right)_p = 2\left(\frac{\partial \ln u_m}{\partial \ln C}\right)_p$$
$$= 1 + j\left[1-\frac{17.7C}{v_c}\right]^{-1}\left\{\frac{17.7C}{v_c}\right.$$
$$\left.\times\left[1+\frac{v_c-17.7C}{12as_m}\right]^{-1}-\frac{\varphi}{1-(\gamma-1)\varphi}\right\}, \tag{43}$$

$$\left(\frac{\partial \ln E_m}{\partial \ln \lambda}\right)_p = 2\left(\frac{\partial \ln u_m}{\partial \ln \lambda}\right)_p = 1 - j\varphi[1-(\gamma-1)\varphi]^{-1}. \tag{44}$$

Similarly if web or burning rate or both are adjusted to maintain the same maximum pressure the effects of varying the chamber volume, v_c or travel, s_m are:

$$\left(\frac{\partial \ln E_m}{\partial \ln v_c}\right)_p = 2\left(\frac{\partial \ln u_m}{\partial \ln v_c}\right)_p$$

$$= j\left[1 - \frac{17.7C}{v_c}\right]^{-1}\left\{\frac{\varphi}{1-(\gamma-1)\varphi} - \left[1 + \frac{v_c - 17.7C}{12as_m}\right]^{-1}\right\}, \quad (45)$$

$$\left(\frac{\partial \ln E_m}{\partial \ln s_m}\right)_p = 2\left(\frac{\partial \ln u_m}{\partial \ln s_m}\right)_p = j\left[1 + \frac{v_c - 17.7C}{12as_m}\right]^{-1}. \quad (46)$$

Finally the change of muzzle energy with maximum pressure, if obtained by changing web or burning rate only, is

$$\frac{\partial \ln E_m}{\partial \ln p_{max}} = 2\frac{\partial \ln u_m}{\partial \ln p_{max}} = j\varphi[1-(\gamma-1)\varphi]^{-1}. \quad (47)$$

Driving Rain Waterproofs Soil.—A rain that soaks the clothing of a person who is out in it may not moisten the ground he is standing on enough to do much good to gardens or crops. But if the land, too, is clothed—say with a sod—the soil beneath may get a good soaking. One soil may be wet by a hard rain and another will not be well soaked unless the rain falls slowly in a drizzle.

U. S. Department of Agriculture investigators are working out the how and why of such situations by tests of soils under artificial rain machines with which they can vary the size of the drops, the speed of fall, and the total fall within a given time. Results furnish basic information useful both in cropping and in wise use of land to prevent erosion.

A recent report by W. D. Ellison of the Soil Conservation Service emphasizes the practical importance of the splash caused by rain falling on bare soil. When a large drop—falling fast—strikes the soil, it splashes; and these splashes are what practically waterproof the surfaces of grain fields and make their soils droughty.

Splashing water may pick up soil particles and set them in motion. If particles are set in motion by the first few splashes, they are carried into the upper layer of the soil with the first water that enters. These fine particles then fill the pores in the soil and block the entry of more water. Thus, a driving rain that splashes and quickly seals the surface does not wet it thoroughly; most of the rain runs off and carries with it other soil particles the driving drops have stirred into motion.

In a drizzling rain, however, with little or no splashing, the pores would remain open; more rain would enter and less run off. Or, if the soil were covered with grass enough to break up the drops before they reached the soil, any slight splashing would not carry many soil particles and would not seal the surface. Thus, soils will be better watered under a pasture than they ever can be under row crops.

Studies of different kinds of soils under artificial rain furnish facts for practical soil management. Such studies cannot change the rainfall, but they indicate the best farming methods for a given soil under the kinds of rain most likely to fall on it.

R. H. O.

NOTES FROM THE NATIONAL BUREAU OF STANDARDS.*

PLASTICS IN GERMANY.

The advances made in the production and application of plastics in Germany during the war period 1939–1945 were surveyed by Gordon M. Kline, chief of the Organic Plastics Section of the Bureau, during a three-months investigation conducted under the auspices of the Office of the Chief of Ordnance, War Department. A report of this survey, a summary of which is given below, was recently issued by the Office of the Publication Board, U. S. Department of Commerce, as publication O.P.B. No. 8, "Plastics in Germany." Important centers of plastics research and development in that country were visited, including the plants of I. G. Farbenindustrie AG. in Ludwigshafen, Leverkusen, Uerdingen, Hochst, and Gendorf; Dynamit AG. in Troisdorf/Koln; Rohm and Haas AG. in Darmstadt; Dr. Alexander Wacker GmbH. in Munich and Burghausen; Th. Goldschmidt AG. in Essen; and Gunther-Wagner in Hannover.

German manufacturing processes and fabricating techniques are well advanced. Their engineers have placed great emphasis on development of continuous processes for the preparation of the raw materials and their conversion into plastics. Four methods of polymerization have been utilized: block or mass, emulsion, pearl or granular, and solution.

Their plastic materials are as diversified as our own, but production is generally on a smaller scale than in the United States. Particularly interesting are the various copolymers which they have found to be useful in such fields as the polyvinyl chlorides, polyacrylates, polyamides, and polystyrenes. Among the new or less well-known polymers which they have been manufacturing are polyvinyl ethers, polyvinyl carbazole, polyethyleneimine, and polyurethanes. In the condensation resin field special compositions and catalysts have been developed for phenolic, urea, melamine, aniline, and alkyd resins. A new resin was prepared during the war from acetylene and butyphenol for use in improving the working properties of synthetic rubber.

A dry-processed unplasticized polyvinyl chloride film, called "Luvitherm," is of particular interest. The polyvinyl chloride is rolled and calendered at 165° C., heated for a few seconds at 260° C., and stretched on a roll heated to 120° C. The film of 1.0 to 1.4 mils thickness cannot be heat-sealed easily because of its high tack point, but can be cemented with cyclohexanone or tetrahydrofurane. An important

* Communicated by the Director.

application is its use as a recording tape, coated with a solution of magnetic iron oxide and a vinyl copolymer. These tapes were in general use on German radio networks and for military communications.

The polyurethanes are a new development in the plastics field and are not on the market in the United States. In general, they are produced by the reaction of polyisocyanates with polyhydroxy compounds such as polyesters. They were in use in Germany for the manufacture of fibers, bristles, adhesives, artificial leather, injection molding compounds, and plastic foams.

The polyvinyl ethers are not made in the United States on a large scale, but were being manufactured in Germany during the war at the rate of approximately 600 tons per month. These polymers are used as lacquer constituents, adhesives, and impregnating agents for paper and textiles.

Polyethyleneimine was made at the rate of about 4 tons per month for use as a paper impregnant. It greatly improves the wet strength and scuff resistance of soft crepe paper. It does not detract from the absorbent qualities; hence it was used for towels, bandages and shoe insoles.

The German army used plastics for many of the same purposes as our own military, for example, signal wire insulation, ammunition fuses, map paper impregnant, gas mask parts, and anti-gas protective clothing. In addition, scarcity of leather, rubber, and other natural products in Germany had led to many civilian uses, such as shoe soles, bicycle tires, motor-drive belts, harness laces, battery cases, artificial leather, and protective coatings.

SURVEY OF ADHESIVES AND ADHESION.

The development of adhesives for bonding metal, wood, rubber, and plastic parts on aircraft has been largely empirical. A better understanding of the physical and chemical forces involved in adhesion is needed for further rational improvement of bonding materials for use in aircraft construction.

Under the sponsorship of the National Advisory Committee for Aeronautics, a research project was undertaken at the Bureau to obtain information on the strengths of bonds between different chemical types of adhesives and adherends. NACA Technical Note No. 989, entitled "Survey of Adhesives and Adhesion," by R. C. Rinker and G. M. Kline, prepared as the initial step in this investigation, comprises a survey of the present knowledge on the nature of adhesion. It includes discussion of (1) the four types of intermolecular and interatomic bonds involved in the attractive forces holding matter together, (2) the chemical and physical forces through which various types of adhesives are attached to solid surfaces, (3) the effects of various factors

on the properties of adhesively bonded structures, and (4) test methods employed for determining tensile and shear bond strengths. A comprehensive bibliography contains references to the technical literature, patents, aircraft and adhesive manufacturers' reports, and reports of the United States and British Governments.

PHYSICAL PROPERTIES OF MICA.

Mica is a strategic material in time of war and is indispensable in many modern peacetime applications. An accurate knowledge of its physical properties is therefore important. A paper by Peter Hidnert and George Dickson in the October *Journal of Research* (RP1675) gives data on the linear thermal expansion, changes in structure, power factors, and effects of heat treatments on thickness, opacity, and color of micas (muscovite, phlogopite, biotite, ripidolite, and zinnwaldite) from different domestic and foreign sources.

The paper gives results of thermal expansion measurements on 30 samples of micas, in a direction perpendicular to the cleavage plane, over the temperature range 20° to 600° or 700° C. Each of the specimens was under load when the measurements were made. Tremendous expansion was noted for some of the samples of phlogopite and biotite micas. Their maximum coefficients of expansion were 0.0552 (between 100° and 114° C.), and 0.00411 (between 500° and 600° C.) per degree C. respectively. The coefficients of expansion of the samples of muscovite, ripidolite, and zinnwaldite micas were comparatively low, the maximum for these three types being 0.000036 per degree C.

Some X-ray diffraction patterns were obtained on a few samples of muscovite, phlogopite, and biotite at room temperature and at elevated temperatures. The transitions shown in the expansion curves of two phlogopite samples and a biotite sample at elevated temperatures, appear to be related to the structural changes indicated in the X-ray diffraction patterns. These changes may be ascribed to the buckling of very thin layers on heating which causes a displacement or tilting of the elementary crystals of the mica laminae.

The power factors of two samples of phlogopite mica from Madagascar and Mozambique were found to be greater at 100 kilocycles than at 1000 kilocycles per second, and considerably larger than the power factors of two samples of muscovite mica from Brazil and Guatemala. Heat treatment of the samples of phlogopite and muscovite micas to 600° C., with or without a load, caused considerable increases in the power factors of the former and only slight changes in the latter.

The effects of heat treatments on the thickness, opacity, and color of 50 samples of various micas, were determined. Nearly all of the muscovite samples showed the greatest increases in thickness (up to 155 per cent.) after heat treatment at 800° C. The results on the

changes in thickness of the phlogopite and muscovite samples indicate that the former resist elevated temperatures better than the latter. The large increases in thickness of nearly all of the muscovite samples accompanied changes from clear or translucent to opaque, or from polychrome to metallic color.

None of the species of mica can be considered as a substance or material of fixed and reproducible properties; there are wide variations in thermal expansion, power factor, and color. These properties of mica depend largely upon the chemical composition, the nature of the crystals, their magnitude and their orientation, the presence of impurities, the way in which these enter the structure, the heat treatment, etc.

Some of the phlogopite and biotite micas, which possess extremely high thermal expansion in a direction perpendicular to the cleavage plane, may be used for high-expanding elements in temperature responsive devices, but on the other hand, may prove unsatisfactory in applications where large changes in dimensions with changes in temperature are not desired.

NEW STANDARDS FOR COLOR AND TINTING STRENGTH OF PAINT PIGMENTS.

Six new standard samples of dry paint pigments suitable for use as standards for color and tinting strength, when such pigments are being purchased on specifications, have been made available since the announcement of the 13 such samples was made in November 1944 (*Technical News Bulletin No. 331*). New Federal Specifications issued recently mention these standard samples, and state that they may be obtained from the Bureau:

NBS No.	Material	Federal Specification
313	Black iron oxide	TT-I-698
314	Yellow iron oxide, light lemon	TT-Y-216
315	Yellow iron oxide, lemon	TT-Y-216
316	Yellow iron oxide, orange	TT-Y-216
317	Yellow iron oxide, dark orange	TT-Y-216
318	Lampblack	TT-L-70

Orders should be sent to the National Bureau of Standards, Washington 25, D. C., and the identifying number and name of the paint pigment wanted should be given. The price per sample is $2.00, payable in advance. Money orders, etc. should be payable to the Bureau.

HYSTERESIS IN THE PHYSICAL ADSORPTION OF NITROGEN ON BONE CHAR AND OTHER ADSORBENTS.

The existence of hysteresis in adsorption phenomena provides evidence that the mechanism of desorption is not, in general, an exact

reversal of the mechanism of adsorption. Since condensation of a vapor on a free liquid surface and the evaporation therefrom is not subject to hysteresis, it is evident that hysteresis in adsorption is to be associated with some peculiarity of the adsorbing surface. An article in the October *Journal of Research* (RP1674) by Leland F. Gleysteen and Victor R. Deitz, research associates at the Bureau representing the United States and Canadian Cane Sugar Refiners and the United States Bone Char Manufacturers, discusses hysteresis in the adsorption and desorption of nitrogen at 77° K. on a new bone char, a spent bone char, an activated carbon, two silica gels, and a coconut-shell charcoal.

It has been found that hysteresis becomes less pronounced in the above adsorbents in the sequence given, occurring only slightly in coconut-shell charcoal and then only after adsorption had been developed at high relative pressures, in the region of which the Langmuir equation is not obeyed. By means of rate measurements it was shown that it is highly probable that a true steady state was attained in the pressure determinations. These rates are compatible with the requirements of diffusion processes and, moreover, were not appreciably different for such adsorbents as bone char and coconut-shell charcoal, which differ widely in the pore sizes attributed to them by many investigators. Consequently, surface migration probably predominates in transporting the adsorbed gas molecules from the immediate exterior of the adsorbent into the more elaborate interior structure. The rate of transport does not differ appreciably for adsorbents of large surface area.

After a discussion of those theories of hysteresis that are based upon the concept of capillary condensation, a new interpretation of hysteresis is presented in terms of the theory of multimolecular adsorption. Hysteresis is associated with the experimental fact that the heat of desorption is greater than the heat of adsorption in the pressure range where the hysteresis is observed. A multimolecular layer of adsorbate may be viewed as one whose similarity to the liquid bulk phase must be complete at saturation pressures. Until that point is reached it is probable that there may be more than one type of configuration possible in the complex structure of the multimolecular layer. Molecular clusters of various sizes may form in adsorption gradually at many points on the adsorbent surface with increasing relative pressures, and eventually these are modified by joining together in some fashion. Subsequently, desorption would occur from adsorbed layers of greater stability. Eventually the desorption and adsorption isotherms join together at sufficiently low relative pressure where the surface is depopulated to the extent where molecular clusters are not stable. These considerations have an advantage over the concepts involved in the capillary condensation theories in guiding fundamental researches in physical adsorption along the modern concepts of molecular structure.

KNOCK RATINGS OF GASOLINE SUBSTITUTES.

Early in the war, Axis submarine packs were able to roam the Atlantic almost at will, preying on United Nations' tankers to such an extent that it appeared probable that shipment of gasoline for non-military use from the United States to neutral or friendly non-belligerent countries might have to be seriously curtailed or discontinued altogether. Foreseeing the effects of such a move on the countries affected, the Foreign Economic Administration (then the Board of Economic Warfare, later the Office of Economic Warfare) charged the Bureau with the problem of investigating the characteristics of materials that might be used as substitute fuels for internal combustion engines (*Technical News Bulletins 339 and 341* (July and September 1945)).

One of the first steps in the survey of the properties and effects of the use of available substitutes was a study of their antiknock qualities. This study, the results of which will be published as RP1673 by Afton D. Puckett in the October number of the *Journal of Research*, included the determination of octane numbers of both liquid and gaseous fuels by current standard test procedures. Carbon monoxide, one of the chief constituents of automotive producer gas, was found to rate well above 100 octane number. The paraffinic gases, from methane through the butanes, were also found to be high in antiknock value, ranging from well above 100 for methane down to 90 ASTM motor octane number for normal butane. All the olefinic gases through C_4 were found to be equal to, or better than, present premium grade motor fuels.

The liquid substitute fuels investigated, listed in order of descending octane number, were acetone, ethyl alcohol, normal butyl alcohol, and diethyl ether. Ether was included in the study, in spite of its known knocking tendency, because of the possibility of using it to improve the volatility of other substitutes. Blends containing varying percentages of ether in ethyl alcohol were found to have somewhat peculiar characteristics, but octane numbers indicated that blends containing ether in amounts less than 45 volume per cent. should give knock-free performance in most present automotive equipment.

Because of the necessity for conserving tetraethyl lead as well as extending gasoline supplies, the amount of ethyl alcohol necessary to raise the knock rating of a 68 motor octane number straight run gasoline to 70 and to 75 motor octane number was determined. With this particular gasoline, 5 volume per cent. and 16.3 volume per cent. respectively of alcohol accomplished these increases in knock rating, as did 0.25 and 1.1 milliliters of tetraethyl lead per gallon. Knock ratings were determined on blends of acetone and ethyl and normal butyl alcohols in a straight run naphtha as well as in gasoline. Although the octane number of acetone exceeds that of ethyl alcohol, it is less effective in blends. Both acetone and ethyl alcohol exhibited lower blending values in a shale-oil motor fuel than in straight run gasolines and naphthas.

THE FRANKLIN INSTITUTE.

STATED MONTHLY MEETING, WEDNESDAY, OCTOBER 17, 1945.

The stated monthly meeting of The Franklin Institute was held at 8:15 on the evening of Wednesday, October 17, 1945. In the absence of the President, Commander W. Chattin Wetherill, Vice-President, presided.

After the playing of the National Anthem, Commander Wetherill introduced Mr. A. F. Daix, 3rd, who spoke briefly on the United War Chest campaign, about to open in Philadelphia. Mr. Daix gave, on a percentage basis, the distribution of the monies collected, and urged the members of the Institute to continue their co-operation in such a worthy project.

After thanking Mr. Daix for his interesting presentation, Commander Wetherill called the meeting to order, and announced that it was the first stated monthly meeting of the season.

He then stated that the minutes of the May meeting had been printed in full in the June JOURNAL, and that unless he heard anything to the contrary, the minutes would be declared approved as printed. There was no dissent.

In the absence of Dr. Henry Butler Allen, Secretary, Dr. John Frazer, Assistant Secretary, was present.

Number of new members added to rolls since the last report in May:

Sustaining	1
Active	259
Associate	156
Student	71
	487
Total membership as of October 1, 1945	5,352

In introducing the speaker of the evening, Dr. Samuel H. Caldwell, Associate Professor of Electrical Engineering, Massachusetts Institute of Technology, Commander Wetherill stated there was no one more capable of discussing his subject, "New Developments in Differential Analyzer Design and Construction," and that in coming to Philadelphia to give the talk, Dr. Caldwell was returning to his native city.

Dr. Caldwell began his talk by stating that in this building (The Franklin Institute) there was fought one of the silent battles of the war—that of research; that science and technology had co-operated wholeheartedly with our fighting men to give them victory, and that The Franklin Institute would be justly proud when its part in the war could be made known.

In discussing his subject, Dr. Caldwell called attention to the work which the scientist and the engineer do to achieve their results, pointing out that it frequently involves highly laborious and tedious methods. His talk described the progress made in applying mass production methods to some of the mathematical problems of science, and told how that progress can be made to accelerate the production of even better living.

The meeting adjourned at 9:50 P.M., but many of the audience remained for further discussion with the lecturer.

JOHN FRAZER,
Assistant Secretary.

COMMITTEE ON SCIENCE AND THE ARTS.

(Abstract of Proceedings of Stated Meeting held Wednesday, October 10, 1945.)

HALL OF THE COMMITTEE,
PHILADELPHIA, OCTOBER 10, 1945.

MR. JAMES D. LEE, JR. *in the Chair.*

The following reports were presented for final action:

No. 3147: Work of Ira Sprague Bowen.

This report recommended the award of a Howard N. Potts Medal to IRA SPRAGUE BOWEN, of Pasadena, California, "In consideration of his brilliant analysis of the problem of the identification of the so-called 'Nebulium' lines, which is based on modern atomic theory and on his own work in the extreme ultra-violet."

No. 3148: Work of Bengt Edlén.

This report recommended the award of a Howard N. Potts Medal to BENGT EDLÉN, of Upsala, Sweden, "In consideration of the light which his researches on the spectra of high excitation ions in the extreme ultraviolet have thrown on the problem of the corona, a contribution which has already stimulated other research on solar problems and promises to influence further work in the field for years to come."

No. 3149: Proportional Spacing Machine.

This report recommended the award of a Certificate of Merit to RONALD D. DODGE, of Poughkeepsie, New York, "In consideration of the skill in design and development of the mechanism in the Proportional Spacing Machine."

LIBRARY NOTES.

The Committee on Library desires to add to the collections any technical works that members would wish to contribute. Contributions will be gratefully acknowledged and placed in the library. Duplicates received will be transferred to other libraries as gifts of the donor.

Photostat Service. Photostat prints of any material in the collections can be supplied on request. Orders received in the morning are filled the same day. The average cost for a print 9 × 14 inches is thirty-five cents.

The library and reading room are open on Mondays, Tuesdays, Fridays and Saturdays from nine o'clock A.M. to five o'clock P.M., Wednesdays and Thursdays from two until ten o'clock P.M.

RECENT ADDITIONS.

ASTRONOMY.

GAMOW, GEORGE. The Birth and Death of the Sun. 1945.

AUTOMOTIVE ENGINEERING.

COHN, DAVID L. Combustion on Wheels. 1944.
MALEEV, V. L. Internal Combustion Engines. Second Edition. 1945.

BIOGRAPHY.

BRODERICK, JOHN T. Willis Rodney Whitney. 1945.

BIOLOGY.

THOMPSON, D'ARCY WENTWORTH. Growth and Form. 1945.

BUILDING.

American Society of Heating and Ventilating Engineers. Transactions 1940–1943, Volumes 46–49. Four volumes. 1942–1944.

CHEMISTRY AND CHEMICAL TECHNOLOGY.

American Gas Association. Proceedings. Twenty-Sixth Annual Meeting. 1944.
BURK, R. E., AND OLIVER GRUMMITT, Editors. Major Instruments of Science and their Applications to Chemistry. 1945.
Electrochemical Society. Transactions. Volume 86. 1945.
LOHSE, HENRY WILLIAM. Catalytic Chemistry. 1945.
MCELVAIN, SAMUEL M. The Characterization of Organic Compounds. 1945.
MCLAUGHLIN, GEORGE D., AND EDWIN R. THEIS. The Chemistry of Leather Manufacture. 1945.
Organic Syntheses. Volume 25. 1945.
WEISSBERGER, ARNOLD, Editor. Physical Methods of Organic Chemistry. Volume 1. 1945.

DICTIONARIES.

SHANKLE, GEORGE EARLIE. Current Abbreviations. 1944.

ELECTRIC ENGINEERING.

DWIGHT, HERBERT BRISTOL. Electrical Coils and Conductors. 1945.
FRAZIER, RICHARD H. Elementary Electric-Circuit Theory. 1945.
KING, RONALD W. P. Electromagnetic Engineering. Volume 1. 1945.
KING, RONALD W. P., HARRY ROWE MIMNO, AND ALEXANDER H. WING. Transmission Lines, Antennas and Wave Guides. First Edition. 1945.

ENGINEERING.

Engineering Index 1944. 1945.

MECHANICAL ENGINEERING.

ECKMAN, DONALD P. Principles of Industrial Process Control. 1945.
PLUMRIDGE, TOM C., ROY W. BOYD, JR., AND JAMES MCKINNEY, JR. Machine Tool Guide. 1945.

METALLURGY AND METAL-WORK.

CARMODY, ELMER J., H. C. LOUDENBECK AND CHARLES E. MACFARLANE. Mixing and Melting Cast Iron. No date.
Institute of British Foundrymen. Proceedings. Volume 37, 1943–1944.
LIDDELL, DONALD M., Editor. Handbook of Nonferrous Metallurgy. Second Edition. 1945.
MANTELL, C. L., AND CHARLES HARDY. Calcium Metallurgy and Technology. 1945.

MILITARY ENGINEERING.

GRAY, GEORGE W. Science at War. 1943.
SMYTH, HENRY DEWOLF. Atomic Energy for Military Purposes. 1945.

PHARMACY.

American Medical Association. New and Nonofficial Remedies. 1945.

PHOTOGRAPHY.

HAMMER, MINA FISHER. The History of the Kodak. 1940.

PHYSICS.

SEARS, FRANCIS WESTON. Principles of Physics, 3. 1945.

RAILROAD ENGINEERING.

KURTZ, C. M. Track and Turnout Engineering. 1945.

SAFETY ENGINEERING.

WOOD, B. L. Fire Protection Through Modern Building Codes. 1945.

SUGAR.

Farr and Company. Manual of Sugar Companies. Twenty-second Edition. 1944.
Louisiana Sugar Manual, 1944–45. 1945.

NOTES FROM THE BIOCHEMICAL RESEARCH FOUNDATION.

Studies on the Chemotherapy of Experimental Virus Infections. II. The Effect of Certain Organic Arsenicals on the Course of Experimental Murine Poliomyelitis.—DONALD W. MCKINSTRY AND ELIZABETH H. READING. The search for drugs effective in altering the course of poliomyelitis has been attended with little success. Innumerable compounds have been studied by many different investigators during the past twenty years with essentially negative results. Sulfonamides (1, 2, 3, 4, 5), sulfones (5), quinoline derivatives (5), hypnotic and convulsive drugs (6a) and dyes (7) have all failed as therapeutic agents. In contradistinction to these entirely negative findings, however, the studies of Jungeblut (6b, c, d) raised hopes for the possibility of influencing the course of the disease favorably by means of chemotherapy. Although none of these promises of therapeutic success has been fulfilled in the clinic, the results have served to encourage further work along this line.

Studies on the chemotherapy of this disease have been seriously handicapped in the past by the fact that experimental infections could be reproduced with certainty only in the *Macacus rhesus* monkey. Unfortunately, in most instances, the number of animals employed was insufficient to permit definite conclusions to be formed regarding the therapeutic value of the compounds studied. Moreover, it has become increasingly evident that simian poliomyelitis is quite different in many important respects from the human disease. Recently, however, Armstrong (8), and Jungeblut and Sanders (9) have succeeded in adapting the virus to rodents. These infections run a true clinical course and the pathology is identical with that found in human poliomyelitis. Furthermore, the rodent can be infected with ease by way of the gastro-intestinal tract and the nasal mucosa which allows simulation of the natural infection. This advance, undoubtedly, will greatly stimulate the systematic search for compounds endowed with antipoliomyelitis properties.

The present investigation deals with the effect of certain organic arsenicals on the course of the experimental murine infection. Investigation of these compounds was prompted by the work of Voegtlin and associates (10) who demonstrated that arsenic exerts its therapeutic action by inactivating functional sulfhydryl groups in certain of the protozoa. In view of the essential role played by these groups in the reproductive process, it was hoped that arsenicals might interfere sufficiently with their action to prevent proliferation of the virus in the host. The rationale of this general method of approach to the study of the chemotherapy of experimental virus infections as well as the

effect of certain pyrimidine derivatives on the course of experimental murine poliomyelitis is given in a previous publication (11).

MATERIALS AND METHODS.

Swiss albino mice, both males and females, weighing 15 to 20 grams each, were employed throughout this study. They were usually held in the laboratory under standard conditions with a balanced diet several days before use. Preliminary studies indicated that these animals were uniformly susceptible to the strains of virus employed and that the infection ran a true clinical course. All of the mice used were from a single source.

The McG, MH and SK rodent strains * of the virus of poliomyelitis were used. These strains, which are highly virulent for mice, produce a typical infection characterized by flaccid paralysis of the extremities which rapidly progresses to a fatal end. Maximal virulence was maintained by frequent mouse passage. Infected brain tissue, aseptically removed from mice sacrificed shortly after the onset of paresis, was used to prepare the inoculum for each test. Several brains were pooled and ground with sterile sand and sufficient 0.1 per cent. glycine to make a 10 per cent. suspension. After refrigeration overnight at 4° C., gross particulate matter was removed by centrifugation at 1500 r.p.m. for 10 minutes. The experimental infections were usually produced by the intraperitoneal injection of 0.1 ml. of the 10^2 dilution (10 to 100 M.L.D.) of a freshly prepared suspension. The virulence of the virus culture employed in each test was determined by titration in mice. The minimum lethal dose was considered to be the smallest amount of virus which killed between 50 and 100 per cent. of the untreated control animals during the observation period of eight days.

Graded doses of the compounds dissolved in sterile distilled water were administered parenterally. The reaction of the suspension or solution was adjusted to pH 7.4 when acidic compounds were used. Ten to fifteen animals with adequate virus controls usually constituted an experimental unit. If a doubtful result was obtained, the test was repeated with a larger number of mice. Preliminary toxicity tests and the frank symptoms of the infection obviated the use of drug controls. Therapy was begun on the day of infection and continued twice daily throughout the observation period. Significant prolongation of life or survival of the treated animals over the controls was used as the criterion of therapeutic potency.

DISCUSSION.

An examination of Table I reveals that certain of the compounds studied exerted a favorable influence against the course of the experi-

* We are indebted to Dr. Claus W. Jungeblut, College of Physicians and Surgeons, Columbia University and to Dr. Gilbert Dalldorf, New York State Department of Health, for the strains of virus employed in this study.

TABLE I.

Effect of Certain Organic Arsenicals on Experimental Murine Poliomyelitis.

Medication				Infection			% Survival		Average Days Survived	
No.	Formula	Dose mg./kg.	Route	Strain	M.L.D.	Route	Treated	Controls	Treated	Controls
1	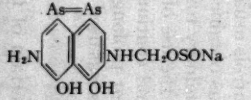	0.1	Subcutaneous	SK	10	Intraperitoneal	20	0	5.9	4.0
		85	Subcutaneous	SK	1–10	Intraperitoneal	30	0	6.3	5.0
		100	Subcutaneous	SK	10–100	Intraperitoneal	50	0	6.6	5.0
		100	Subcutaneous	MH	10–100	Intraperitoneal	10	0	4.7	5.0
		100	Subcutaneous	SK	100	Intranasal	40	0	6.1	4.0
		100	Subcutaneous	SK	10	Per os	10	0	6.8	4.0
		100	Subcutaneous	McG	1–10	Intracerebral	20	0	16.0	15.4
		167	Intraperitoneal	SK	10	Intraperitoneal	20	0	4.8	4.5
2		25	Subcutaneous	SK	100	Intraperitoneal	0	0	1.3	5.0
3	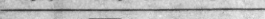	0.1	Subcutaneous	SK	10–100	Intraperitoneal	0	0	4.7	3.0
4	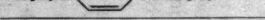	0.1	Subcutaneous	SK	10–100	Intraperitoneal	0	0	4.0	4.0
5	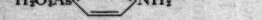	140	Subcutaneous	SK	10	Intraperitoneal	0	0	3.8	3.5
6	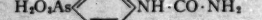	50	Subcutaneous	SK	10	Intraperitoneal	0	0	5.3	2.5
7		5.0	Subcutaneous	SK	10	Intraperitoneal	20	0	5.2	4.0
		10.0	Subcutaneous	SK	10	Intraperitoneal	20	0	5.9	4.5
8		0.1	Subcutaneous	SK	10	Intraperitoneal	0	0	4.4	4.0
9	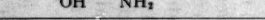	0.1	Subcutaneous	SK	10–100	Intraperitoneal	10	0	5.0	4.0
		100	Subcutaneous	SK	10	Intraperitoneal	20	0	5.5	3.5

Table I—(*Continued*).

Medication				Infection			% Survival		Average Days Survived	
No.	Formula	Dose mg./kg.	Route	Strain	M.L.D.	Route	Treated	Controls	Treated	Controls
10	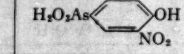	0.1 100	Subcutaneous Subcutaneous	SK SK	10 10	Intraperitoneal Intraperitoneal	10 20	0 0	4.8 6.0	3.5 3.5
11	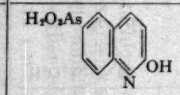	0.1	Subcutaneous	SK	10	Intraperitoneal	0	0	4.8	5.0
12	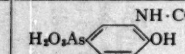	10 100 100	Subcutaneous Subcutaneous Subcutaneous	SK SK SK	10 10–100 100	Intraperitoneal Intranasal Intraperitoneal	40 20 50	0 0 0	5.7 5.1 6.2	4.0 3.5 5.0
13		0.1 10	Subcutaneous Subcutaneous	SK SK	10 10–100	Intraperitoneal Intraperitoneal	0 30	0 0	5.0 5.5	4.0 3.5
14	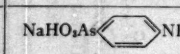	500 1000 2000 2000	Subcutaneous Subcutaneous Subcutaneous Subcutaneous	SK SK SK SK	10 10 10 1000	Intraperitoneal Intraperitoneal Intraperitoneal Per os	30 20 20 50	0 0 0 0	6.1 5.0 6.5 6.2	3.5 3.5 3.5 4.0
15	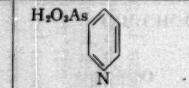	125	Subcutaneous	SK	10	Intraperitoneal	0	0	2.6	3.5
16	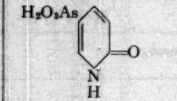	0.1	Subcutaneous	SK	10	Intraperitoneal	10	0	4.2	4.0

TABLE I—(*Continued*).

Medication				Infection			% Survival		Average Days Survived	
No.	Formula	Dose mg./kg.	Route	Strain	M.L.D.	Route	Treated	Controls	Treated	Controls
17	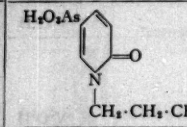	0.1	Subcutaneous	SK	10–100	Intraperitoneal	0	0	4.4	4.0
18	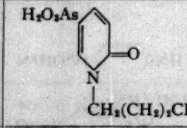	50	Subcutaneous	SK	10	Intraperitoneal	0	0	4.1	4.0
19	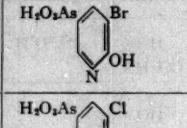	100 250	Subcutaneous Subcutaneous	SK SK	10 10	Intraperitoneal Intraperitoneal	10 20	0 0	4.6 5.0	3.5 4.0
20	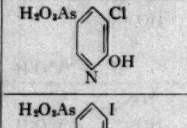	0.1 100	Subcutaneous Subcutaneous	SK SK	10 10	Intraperitoneal Intraperitoneal	10 10	0 0	4.7 5.8	4.0 3.5
21	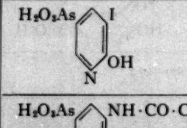	0.1 100	Subcutaneous Subcutaneous	SK SK	10 10	Intraperitoneal Intraperitoneal	0 10	0 0	3.9 4.8	5.0 3.5
22	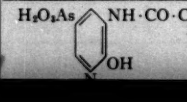	0.25	Subcutaneous	SK	10–100	Intraperitoneal	0	0	4.4	3.0

mental infection. Eight of the drugs protected a significant percentage of the mice from infection with 10 to 100 M.L.D. of the virus and prolonged the life of the remainder. Neoarsphenamine, No. 1, stovarsol, No. 12, and tryparsamide, No. 14, the most effective compounds studied, regularly prevented paralysis and death in from 20 to 50 per cent. of the cases and markedly ameliorated the symptoms in the others. Relatively large doses of the arsenicals were required, however, to bring about this therapeutic action. Arsacetin, No. 7, 3-amino-4-hydroxy-phenylarsonic acid, No. 9, 2-hydroxy-3-bromopyridine-5-arsonic acid, No. 19, 2-hydroxy-3-chloropyridine-5-arsonic acid, No. 20, 3-nitro-4-hydroxy-phenylarsonic acid, No. 10, and Mapharsen, No. 13, were somewhat less effective. The other compounds either exerted no effect or only slightly prolonged the life of the treated animals over that of the controls. Neoarsphenamine was effective against all three strains of virus studied and significant numbers of animals were protected regardless of the route by which the virus was administered.

The data presented in Table II show the antagonistic effect of

TABLE II.

Effect of Glutathione and Cysteine on the Antiviral Action of Neoarsphenamine.

Antagonist		Neoarsphenamine Dose Subcutaneously mg./kg.	Infection Produced by SK Strain. Intraperitoneally M.L.D.	% Survival		Average Days Survived	
Compound	Dose Intraperitoneally mg./kg.			Treated	Controls	Treated	Controls
Glutathione	153[1]	114[2]	10	30	0	5.9	5.0
	—	114	10	45	0	7.3	5.0
	768[3]	114	10	0	0	4.7	7.0
	—	114	10	35	0	7.6	7.0
Cysteine·HCl	79.13[1]	114	10	13	0	5.3	5.0
	—	114	10	45	0	7.3	5.0
	395.6[3]	114	10	0	0	1.8	4.0
	—	114	10	30	0	6.3	4.0

[1] 0.5 millimoles per kilo.
[2] 0.25 millimoles per kilo.
[3] 2.5 millimoles per kilo.

cysteine and glutathione on the antiviral action of neoarsphenamine. The action of the arsenical at a dosage of 0.25 millimoles per kilo per day was completely nullified by the administration of 2.5 millimoles per kilo per day of either of the antagonists. When the infection was treated with a 2 to 1 molar ratio of antagonist and neoarsphenamine, however, the therapeutic action of the arsenical was only slightly affected. These data seem to indicate that the arsenical may have exerted its antiviral action by interfering in some manner with the sulfhydryl system in the host-parasite interaction.

TABLE III.

Effect of Massive Doses of Neoarsphenamine with Various Detoxicants on Experimental Murine Poliomyelitis.

Detoxicant		Arsenical Dose Subcutaneously mg./kg.	Infection Produced by SK Strain. Intraperitoneally M.L.D.	% Survival		Average Days Survived	
Compound	Dose Intraperitoneally mg./kg.			Treated	Controls	Treated	Controls
Ascorbic Acid	350	300	1	0	50	3.8	7.5
	800	200	100	0	0	3.9	5.0
	800	150	10	13	0	4.7	4.0
p-Aminobenzoic Acid	1200	300	1	0	50	3.8	7.5
	1600	200	100	0	0	3.3	5.0

Table III gives the results obtained with massive doses of neoarsphenamine in combination with ascorbic acid and *p*-aminobenzoic acid. Unfortunately, neither compound was effective in reducing the toxicity of the arsenical to a safe level.

The result of efforts to potentiate the action of neoarsphenamine with a number of unrelated compounds is given in Table IV. Exami-

TABLE IV.

Effect of Neoarsphenamine with Certain Supplemental Drugs on Experimental Murine Poliomyelitis.

Supplemental Drug			Arsenical Dose Subcutaneously mg./kg.	Infection Produced by SK Strain. Intraperitoneally M.L.D.	% Survival		Average Days Survived	
Name	Dose mg./kg.	Route			Treated	Controls	Treated	Controls
Mercurochrome	50	Intravenous	50	1	7	50	4.5	7.0
Fouadin	100	Intraperitoneal	75	10	53	0	7.1	4.5
Sulfapyridine	50[1]	Per os	75	10	53	0	7.0	4.5
Sulfadiazine	50[1]	Per os	100	10	10	0	5.7	6.0
Safranine Bluish	10	Intraperitoneal	75	10	10	0	5.3	4.5
Induline R	75	Intraperitoneal	75	10	10	0	5.1	4.8
Ethyl 2-Oxo-4-phenyl-6-methyl-1,2,3,4-tetrahydro-5-pyrimidine-carboxylate	50[1]	Per os	100	10	10	0	4.9	4.5

[1] Administered by gavage twice daily.

nation of these data shows that fouadin and sulfapyridine appeared to enhance the action of the arsenical to a very slight extent. The other compounds were without effect.

A typical protocol is given in Table V.

Summary. Three of twenty-two organic arsenicals studied exerted a slight effect against the course of experimental murine poliomyelitis

TABLE V.

Effect of Neoarsphenamine with Certain Supplemental Drugs on the Course of Experimental Murine Poliomyelitis.

Drugs	Medication			Dil.[1] of Virus	No. of Mice	Death of Mice (Days)								Mice Surviving 8 Days	Average Days Survived[2]
	Arsenical Dose Subcutaneously mg./kg.	Supplement				1	2	3	4	5	6	7	8		
		Dose mg./kg.	Route												
Safranine Bluish + Neoarsphenamine	75	10	Intraperitoneal	10^2	10					4	3		2	1	5.3
Induline R + Neoarsphenamine	75	75	Intraperitoneal	10^2	10					5	3			2	5.1
Fouadin + Neoarsphenamine	75	100	Intraperitoneal	10^2	15						3		4	8	7.1
Sulfapyridine + Neoarsphenamine	75	50[3]	Per os	10^2	15						4		3	8	7.0
Virus Controls				10^2	4				1	1	1	1	—	0	4.5
				10^3	4						2			2	6.5
				10^4	4						1		1	2	7.0

[1] 0.1 ml. SK murine poliomyelitis virus No. 335 administered intraperitoneally.

[2] $\frac{\text{number of mice} \times \text{days each survived}}{\text{total number of mice}}$ calculated for the observation period of 8 days.

[3] Administered twice daily.

as indicated by prolongation of life of the treated animals over that of the controls.

The therapeutic action of neoarsphenamine, one of the most effective compounds studied, was antagonized by cysteine and glutathione.

Fouadin and sulfapyridine appeared to enhance the antiviral action of neoarsphenamine to a very slight extent.

REFERENCES.

(1) KELSON, S. R., *Proc. Soc. Exptl. Biol. Med.*, 36, 718 (1937).
(2) MCKINLEY, E. B., ACREE, E. G., AND MECK, J. S., *Science*, 87, 43 (1938).
(3) TOOMEY, J. A., AND TAKACS, W. S., *Arch. Pediat.*, 55, 307 (1938).
(4) RHODES, A. J., AND VAN ROOYEN, C. E., *Brit. Med. J.*, 1, 924 (1938).
(5) COGGESHALL, L. T., AND MAIER, J., *J. Pharmacol.*, 76, 161 (1942).
(6) JUNGEBLUT, C. W., a. *Proc. Soc. Exptl. Biol. Med.*, 43, 464 (1940).
JUNGEBLUT, C. W., b. *Proc. Soc. Exptl. Biol. Med.*, 28, 176 (1930–31).
JUNGEBLUT, C. W., c. *J. Bact.*, 31, 34 (1936).
JUNGEBLUT, C. W., d. *J. Exptl. Med.*, 70, 315 (1939).
(7) HORNUS, G., AND HABER, P., *Compt. rend. soc. biol.*, 117, 656 (1934).
(8) ARMSTRONG, C., *Pub. Health Rep.*, 54, 1719 (1939).
(9) JUNGEBLUT, C. W., AND SANDERS, M., *Proc. Soc. Exptl. Biol. Med.*, 44, 375 (1940).
(10) VOEGTLIN, C., DYER, H. A., AND LEONARD, C. S., *Pub. Health Rep.*, 38, 1882 (1923).
(11) MCKINSTRY, D. W., AND READING, E. H., *J. Franklin Inst.*, 237, 422 (1944).

PUBLICATIONS RECEIVED.

The Chemical Constituents of Petroleum, by A. N. Sachanon. 451 pages, tables and illustrations, 16 × 23 cms. New York, Reinhold Publishing Corporation, 1945. Price $8.50.

Bioenergetics and Growth with Special Reference to the Efficiency Complex in Domestic Animals, by Samuel Brody. 1023 pages, illustrations, 16 × 24 cms. New York, Reinhold Publishing Corporation, 1945. Price $8.50.

L'Azéotropisme, la Tension de Vapeur des Melanges de Liquides. Bibliographie. Par Maurice Lecat. viii + 123 pages, 16 × 25 cms., paper. Bruxelles, Maurice Lamertin, Editeur, 1942.

Advancing Fronts in Chemistry, Volume I, High Polymers, edited by Sumner B. Twiss. 196 pages, illustrations, 15 × 23 cms. New York, Reinhold Publishing Corporation, 1945. Price $4.00.

A War Job "Thought Impossible," by Wesley W. Stout. 51 pages, illustrations, 13 × 21 cms. Detroit, Chrysler Corporation, 1945.

CURRENT TOPICS.

ARMY AND NAVY NOTES.

Under-Channel Oil Line.—How American productive capacity and technical know-how aided the British government in achieving a modern engineering wonder, the laying of 20 three-inch oil pipe lines under the English Channel to supply Allied armies with oil soon after they landed on the Normandy coast, has been revealed by engineers of General Electric, one of the four American concerns that produced sizable quantities of the pipe for our British ally.

The project of piping oil under the Channel to supply an Allied fighting machine doing battle on another continent, was conceived by Lord Louis Mountbatten in April, 1942. Since then, the lines have carried an average of 1,000,000 gallons a day, it was revealed in a report from Geoffrey Lloyd, Minister of the British Petroleum Warfare Department.

To American industrial plants which were given the momentous job of adding their great productive capacity to that of Britain, the project presented difficulties never before encountered. Average cables previously manufactured had an internal pressure of from 10 to 15 pounds per square inch; the new line demanded pipes that could withstand pressures of 1,200 pounds per square inch.

General Electric, because of its technical knowledge and high production standard, was given a contract to manufacture 20 miles of the new pipe line on March 3, 1944, and got into production on the project on June 1. Twelve days later the first shipment was ready to be sent overseas for installation. With more than 25,000 feet of the pipe included in each shipment, G.E. produced four shipments of the pipe. The last of these contracted for was completed on July 17 in only 10 days time, an average of more than 3,000 feet per day.

Because the undersea pipe line was designed to withstand tremendous internal pressures, new methods of manufacture had to be set up on a moment's notice. A. C. Hartley, British engineer, who was instrumental in drawing up the original plans, came to America to collaborate with engineers here in reconverting their plants and retraining their technicians. Separate shifts worked around the clock, old machinery was reconverted, while production was going on, to do new jobs. Jobs that previously required several weeks to complete were accomplished in a single day.

According to V. A. Sheals, G-E design engineer on the job, a production line more than 400 feet long was finally set up at General Electric. Here workmen and engineers who, because of secrecy orders, did not know what they were working on, aided considerably in accomplishing a miracle that might have turned the tide of the war.

The Engineers Corps, United States Army, collaborated with G.E. and other American firms in manufacturing the heavy-duty pipe.

R. H. O.

Fiberglas Tower Packing Helps Atlantic Engineers Speed Production of High Octane Gasoline.—When The Atlantic Refining Company some three years ago undertook volume production of 100-octane gasoline from high-sulphur-content oil the company's engineers were confronted with a serious production "bug."

Enormous quantities of aviation fuel were urgently needed by our own armed forces and those of our allies. New refinery equipment was difficult to obtain, but engineers at Atlantic's Philadelphia refinery succeeded in adapting old equipment to the process.

The "bug" was due in part to this use of equipment which was not designed for the job, and in part to the chemical composition of the high-sulphur-content oil which had long been considered unsuitable for production of 100-octane gasoline.

The production process involves passing oil vapor through a catalyst, under pressure. The catalyst chamber is approximately 25 feet high and 6 feet in diameter. The vapor enters the chamber at the top, passes through the catalyst, and out at the bottom.

The "bug" was eliminated by a combination of engineering ingenuity and a hitherto untested use by Atlantic of Fiberglas Tower packing. It—the "bug"—reared up when it was discovered that the mixture of iron sulphide, scale, coke and carbon particles entrained in the vapor quickly formed a crust in the top stratum of the catalyst that prevented a free flow of the vapor.

Flow could be maintained only by steadily increasing the pressure. When the pressure limit was reached it was necessary to clean out and repack the chamber with new catalyst, even though the old catalyst was still active.

It was decided that what was required to filter out the particles, and at the same time permit a free flow of vapor for a maximum period, was an inert tower packing material of the proper physical structure.

Fiberglas packs were selected as the logical material because Fiberglas is inert, because the glass fibers are non-hygroscopic, and because of the very large surface area. A single layer of Fiberglas packs, 3 inches thick, with a density of one and a half pounds per cubic foot, and with a surface area of 537 square feet per pound of glass, was laid over the top of the catalyst.

The glass fiber filter proved completely satisfactory. Experience has shown that the interlaced glass fibers entrap the entrained particles, but permit a free flow of vapor for a longer time than the catalyst itself remains active.

Clogging has ceased to be a reason for cleaning out and repacking the catalyst chamber. Cleaning and repacking is necessary only when the catalyst is exhausted. At such times the used Fiberglas packs are discarded, and new ones are installed.

Use of the Fiberglas tower packing has at least doubled the length of the run, according to Atlantic's engineers, and has materially speeded production of much-needed high-octane aviation fuel.

R. H. O.

New Portable Tube X-Rays Warplane Wings.—In order to examine internal structure of welds, rivets and other vital points of stress in confined spaces such as airplane wings, fuel tanks, etc., North American Philips Com-

pany recently introduced this new X-ray unit which is now at work in several aircraft plants.

The shockproof tube (approximately 3" in diameter) is coupled to the generator by means of a shockproof cable and two small water hoses. Water cooling makes possible the compact design so useful for analysis on completed structures.

In use, the X-ray tube is clamped to (or held against) the section under examination. Standard X-ray film is then placed on the opposite side of the area and the exposure is made. The high-loading-anode tubes are available with targets of copper cobalt, iron, or molybdenum. Ratings range from 10 to 20 ma at potentials up to 50 kvp, depending on the target material.

The main generator may be mounted on a dolly for movement to certain stations where electrical and water connections are available. It may also be assigned to a fixed location where parts are brought within reach of the tube.

Controls include a stepless kilovoltage regulator, filament rheostat, circuit breaker (serving as main control), and a high-voltage pushbutton switch. A milliammeter is provided for proper adjustment of tube current and a running-time meter records tube life. The pilot light shows when the tube is energized. There is an outlet to permit use of an exposure timer. Doors of the black, crackle-finished cabinet have safety switches on the high voltage circuit.

R. H. O.

Bullets for War.—When General Eisenhower's plea for more ammunition shocked the United States out of its state of complacency in late November 1944, the War Production Board promptly called on the Western Electric Company to help in an all-out effort to rush those sorely needed bullets to our fighting men. True, a great many people may wonder how the country's largest manufacturer of electronic and communications equipment would fit into an accelerated bullet production program, but the answer is quite simple.

At its great Hawthorne Works, near Chicago, Western Electric maintains one of the nation's most modern metals fabricating mills. Although not large when compared with some of the country's huge ordnance plants, having a limited capacity of approximately a million and a quarter pounds of metal a month, its special output of gilding metal for use in 0.30 and 0.50 caliber bullet jackets certainly proved significant in helping to meet the Western Front emergency. In normal times this mill produces a wide variety of magnetic and non-ferrous metals required in the production of peacetime telephone equipment. However, in the last three years it has supplied these materials for use by Western Electric in the manufacture of combat equipment for the Armed Forces.

The gilding metal produced at the Hawthorne mill consists of an alloy of 90 per cent. copper and 10 per cent. zinc with an impurity content of less than ten per cent. so as not to impair forming characteristics necessary in the fabrication of bullet jackets. Starting off as copper ingots and zinc slabs, or as high grade scrap of known composition, the metals are melted down and cast into bars. The bars are cold rolled, annealed and milled, then cold rolled into strips and, after an intermediate annealing and pickling operation are finally cold rolled to a thickness of 0.041 of an inch. These long strips are annealed and pickled, then slit into 5-inch widths, coiled, and shipped to an

ordnance plant for further processing. At the ordnance plant the metal is "blanked" and "cupped" in preparation for further processing at other ordnance plants which draw, shape, and fit the gilding metal cups with steel inserts. Finally the bullet is inserted into the shell case complete with powder.

The production of gilding metal at the mill runs approximately 700,000 pounds a month which is sufficient for about 40,600,000 bullet jackets. Under this schedule, 400,000 pounds go into 0.30 caliber bullets while the other 300,000 pounds are used for 0.50 caliber bullets.

R. H. O.

Florida Rubber Trees.—Rubber production from native plants in southern Florida is not promising at present, and commercial plantings of tropical rubber plants there would not now be justified, in the opinion of rubber specialists of the U. S. Department of Agriculture. A Florida Everglades rubber production project has been advocated recently as a benefit for returning veterans.

Veterans, according to the Department's understanding of the proposal, would be given 25 to 50 acres of the Everglades and encouraged to plant rubber trees for future supplies of natural rubber in the United States.

Rubber plant investigations, it is pointed out, are being conducted by the Department in various parts of the United States and in Latin America, but the results to date show that commercial development of such plantings in Florida at present would be premature and hazardous.

The Florida studies, over a period of more than 20 years, have included the introduction of many rubber-bearing plants, including the Para rubber tree, the Central American rubber tree, the African rubber tree, and the Ceara rubber tree, but the growth of these trees has been slow and the rubber yields low. Cold damage has been severe except in well protected locations.

The strangler fig, best of the native trees investigated, does not respond well to tapping and yields a latex with only 2 to 3 per cent. rubber as compared to the latex of the Para rubber tree which contains 30 to 45 per cent. Strangler fig production has thus been shown to be unprofitable under present or normal conditions.

"In Florida it would not now be possible," says the Department, "to compete with tropical areas where conditions are favorable for rapid growth and high yields, and where wage rates are much lower. Until the Nation's first-line sources and second line reserves of rubber are assured, research looking toward domestic production must continue, but unjustified claims or premature developments, such as that suggested for the Florida Everglades, cannot but becloud the issue."

R. H. O.

New Process for Making Ethyl Chloride.—A new process for making ethyl chloride, one of the most important chemicals used in manufacturing Ethyl fluid to produce high octane gasoline powering allied air fleets on the world's battlefronts, is announced by Ethyl Corporation. A $750,000.00 unit employing this process is now under construction at the company's Baton Rouge, La. plant.

The process yields ethyl chloride by reacting chlorine with waste products from one of the present ethyl chloride units at Baton Rouge. It was developed in view of the "tight" supplies of both alcohol and ethylene, compounds used in producing ethyl chloride, through two present processes.

The principal use of ethyl chloride is in making tetraethyl lead by combining it with an alloy of lead and sodium. Tetraethyl lead comprises about two-thirds of Ethyl fluid and does the work in taking out the "knock" in gasoline.

Ethyl chloride also is used in dentistry as an anesthetic on abscessed gums, as a general anesthesia in short operations with the advantage of no after-effects, in producing ethyl cellulose which is the basis for certain plastics, as a catalyst in synthetic rubber manufacture, as a constituent of cognac essence and sometimes as a refrigerant.

Because of the enormous amounts used in making tetraethyl lead, Ethyl Corporation is the world's largest producer and consumer of this chemical compound.

Chlorine for the new process is produced by breaking salt electrically into chlorine and sodium. The sodium from this electrolysis is combined with metallic lead to form a lead-sodium alloy used in making tetraethyl lead.

The two methods already in operation for making ethyl chloride are based (1) on the hydrochlorination of alcohol, and (2) on the hydrochlorination of ethylene. In the alcohol process, ethyl alcohol vapor and hydrochloric acid combine in the presence of a catalyst to form ethyl chloride and water.

In the ethylene process, ethylene gas is mixed with hydrogen chloride gas in the presence of a catalyst. The two gases first are passed through a reactor where hydrochlorination occurs, and later through a "flash drum" which distills off the lighter ethyl chloride fractions, leaving the heavier polymer fractions. The ethyl chloride then is purified by fractionation. The first of two plants using the ethylene process was built in 1939.

The new process was developed because of increasing wartime demands for raw materials. Before the war, Ethyl Corporation converted all the chlorine from electrolysis of salt to hydrogen chloride to make ethyl chloride, and brought additional amounts of chlorine elsewhere. Due to rising wartime demands for tetraethyl lead and for chlorine in other uses, the company overproduced sodium in 1941 to obtain more chlorine, discontinuing open market purchases of chlorine, and storing the surplus sodium.

When nationwide chlorine supplies became critically short, Ethyl Corporation expanded its plant facilities to substitute hydrochloric acid for chlorine, producing the hydrochloric acid from sulphuric acid and common salt.

Then ethyl alcohol, used in making detonating powders and butadiene for synthetic rubber, came increasingly into demand. Construction of a second ethylene plant at Baton Rouge for the production of ethyl chloride helped to relieve the supply situation in ethyl alcohol.

As the war progressed, supplies of ethylene in the Baton Rouge area became inadequate in meeting the continuously increasing demands for ethyl chloride needed to manufacture Ethyl fluid for the war effort. When the new plant is in production, Ethyl Corporation expects to meet all increased requirements for ethyl chloride for tetraethyl lead without additional drain upon available supplies of alcohol or ethylene.

R. H. O.

A Foreign Vacuum Tube.—Included among the spoils of war which accrued to General Omar S. Bradley's fighting army, as it swept across France, Belgium and Germany, was the partially wrecked strategic Belgian telephone communications system. A hasty check revealed that the ferocity of the American attack had given the Nazi demolition squads little time for action. Most of the equipment was intact—Signal Corps men at testboards in repeater stations okayed line after line as the splicers brought them in—but then the real trouble was discovered; there was not a single vacuum tube in a socket and none in stock. However, a ray of hope soon developed; someone discovered and interviewed a tubemaker in the vicinity who knew some of the characteristics of the tube. Someone else uncovered a carefully wrapped package tucked away in a corner; it contained a single vacuum tube. So the tube and the penciled notes were rushed to New York by plane, and on a Wednesday afternoon in mid-December they were in the hands of the design engineers of Bell Telephone Laboratories.

The odd little German-made repeater tube was covered with an opaque coat of sprayed metal, making visual inspection of its internal elements impossible without injury to the tube, but electrical tests quickly told its characteristics; fortunately, they coincided with the information in the notes. Working late that night the Bell Laboratories' scientists roughed out the design of a tube which duplicated the characteristics of the German tube. The design was such that parts of certain Western Electric carrier-repeater tubes, available in stock, could be used except for the bases and one of the grids. That night the Tube Development Shop wound some grids and drilled a few bases to accommodate the proper size pins.

In the meantime the Western Electric Company's Tube Shop at Hudson Street had been notified, and prepared to go into immediate production on over a thousand of these urgently needed vacuum tubes. Thursday morning found the job underway in the Tube Shop, and by Monday the first package of eight tubes, replicas of a German tube, different not only in dimensions but also in electrical characteristics from any vacuum tube previously manufactured in this country, was on its way to Europe. Production on the remainder continued on a rush basis and in less than two weeks the entire lot of over a thousand tubes had been completed and shipped by air to the fighting front.

The unique design of the tube presented many manufacturing problems, one of which was the metal spray on the surface of the tube which is electrically connected to a nickel shield around the circumference of the base. However, it was soon discovered that a zinc spray would more satisfactorily do the job than aluminum which was used on the first samples. Testing and aging offered another problem but by making use of available equipment at both the Laboratories and the Tube Shop this problem was licked. Some time later one of the Laboratories' technical observers in the European Theatre sent the welcome news that the tubes were doing their job satisfactorily.

For a job well done expressions of thanks were received in letters from Major General H. C. Ingles, Chief Signal Officer, and from Dr. Vannevar Bush, Director of the Office of Scientific Research and Development. Dr. Bush wrote: "Your part in the spectacular job accomplished under our contract providing the tube represents a record-breaking performance and merits the

sincere praise and thanks of this organization and those who will use the equipment."

R. H. O.

Motion Picture, Radio and Television Industries May Benefit from War-Developed Fiberglas Sound Control Materials.—Hollywood, May 18—A basis for the development of products that will meet the sound control requirements of the motion picture, radio and television industries is provided by the Fiberglas noise absorbing materials developed during the war period for use in military aircraft, Willis M. Rees, acoustical specialist of Owens-Corning Fiberglas Corporation, told the society of Motion Picture Engineers, recently.

In his discussion of the acoustical properties of Fiberglas, which was prepared jointly by Mr. Rees and Robert B. Taylor of the Fiberglas Research Laboratories, Mr. Rees stated that the most recent development is a down-like fiber of submicroscopic fineness which is made into incombustible aircraft blankets with exceptional heat and sound insulating properties, combined with extremely light weight and low moisture absorption. The average diameter of one type of these down-like fibers is five hundred-thousandths (0.00005) of an inch. Blankets composed of these fibers and weighing two and a half ounces per square foot are being used for sound insulation in multi-motor heavy bombers.

"It has been stated," Mr. Rees said, "that friction of pulsating air molecules against the walls of the interstices of porous materials dissipates sound energy into heat, and that it is in this way that most sound absorption is provided. Within limitations, the greater the surface area provided by these interstice walls, the greater the sound absorption. There is a tremendous increase in the square foot surface area of a pound of Fiberglas as the fiber diameter decreases. Further research may demonstrate that acoustical values are functions of the fiber diameter and of the surface area of the fibers that make up the material."

While stating that there are not yet enough data on which to base scientific conclusions, Mr. Rees pointed out that Fiberglas materials provide a group of incombustible products apparently subject to more complete control than has ever before been possible in acoustical research.

"With control of thickness, density, fiber diameter and surface area per unit of volume or weight; with possible control of resilience, porosity of surface films, and combinations with perforated surfaces; and with control of methods of mounting and assembling materials in actual use, the conclusion is warranted that research men can find in Fiberglas materials the means of conducting basic research in the physics of sound absorption that will lead to development of sound control products much needed by the motion picture, radio and television industries," he said.

R. H. O.

Orlando Scientists Develop New Insect Repellents.—Development by entomologists of the U. S. Department of Agriculture of new insect repellents, effective against mosquitoes and chiggers, and to a lesser extent against wood ticks, may now be revealed. These repellents, which include dimethyl phtha-

late, have been used extensively by the allied armies since 1942. They are not yet available for civilian use.

In May, 1942, when dimethyl phthalate was tested at the Orlando (Fla.) laboratory as a repellent against mosquitoes, it was found to be more effective for preventing bites of the malaria mosquito, *Anopheles quadrimaculatus*, than any other compound known at that time. Immediately after it was found to be safe for use on the skin of man by the Pure Food and Drug Administration, it was made available to the armed forces, where it was urgently needed. The information developed by the Bureau of Entomology and Plant Quarantine and the Food and Drug Administration served as the basis for such early use of dimethyl phthalate as it was already in production for civilian use (for other purposes) and could be manufactured with existing equipment.

Later, an improved mosquito repellent using dimethyl phthalate as one of the ingredients was developed at the Bureau's Orlando laboratory. It was found that six parts of dimethyl phthalate, two parts of indalone, and two parts of 2-ethyl hexanediol was just as effective for malarial mosquitoes found in this country as dimethyl phthalate, and that the mixture was more effective for a variety of mosquitoes and biting flies than the pure dimethyl phthalate. This development has enabled the armed forces to issue a single repellent for the protection of personnel against a variety of insects.

In 1942, research workers, A. W. Lindquist and A. H. Madden, tested many materials, including dimethyl phthalate, against mites known as "chiggers." It was found that dimethyl phthalate, as a liquid insect repellent, when properly applied to clothing assured that the person using it would be safe from mite or chigger attack. This repellent is applied lightly to the inside of the cuff of trousers and sleeves as well as the buttoned surfaces of the shirt. This barrier prevents chiggers from crossing it and attaching to the skin of man. It kills the ones that are not repelled by it.

In early tests several hundred soldiers on maneuvers in Louisiana found that a single treatment of dimethyl phthalate was effective for at least two weeks, and in many cases for more than four, while some of those wearing untreated clothing received such severe bites they had to be hospitalized. Since then, dimethyl phthalate has been used extensively and with great success against chiggers by allied military forces in the Pacific theaters.

When dimethyl phthalate is emulsified and used in the treatment of the outer garments, it gives protection against chiggers between launderings or for almost a month with unwashed clothing. It is not effective, however, on clothing worn in the water, as when troops have to wade. Light sprays of this compound were applied also to the trousers below the knee, where they were effective in preventing attachments of immature stages of ticks. It is not completely effective against adult ticks, but does afford a degree of protection.

R. H. O.